
Rethinking Symbolic Regression Datasets and Benchmarks for Scientific Discovery

Yoshitomo Matsubara*

Amazon Alexa AI

yoshitom@uci.edu

Naoya Chiba

OMRON SINIC X Corporation

naoya.chiba@sinicx.com

Ryo Igarashi

OMRON SINIC X Corporation

ryo.igarashi@sinicx.com

Tatsunori Taniai

OMRON SINIC X Corporation

tatsunori.taniai@sinicx.com

Yoshitaka Ushiku

OMRON SINIC X Corporation

yoshitaka.ushiku@sinicx.com

Abstract

This paper revisits datasets and evaluation criteria for Symbolic Regression, a task of recovering mathematical expressions from given data, specifically focused on its potential for scientific discovery. Focused on a set of formulas used in the existing datasets based on Feynman Lectures on Physics, we recreate 120 datasets to discuss the performance of symbolic regression for scientific discovery (SRSD). For each of the 120 SRSD datasets, we carefully review the properties of the formula and its variables to design reasonably realistic sampling ranges of values so that our new SRSD datasets can be used for evaluating the potential of SRSD such as whether or not an SR method can (re)discover physical laws from such datasets. As an evaluation metric, we also propose to use normalized edit distances between a predicted equation and the ground-truth equation trees. While existing metrics are either binary or errors between the target values and an SR model’s predicted values for a given input, normalized edit distances evaluate a sort of similarity between the ground-truth and predicted equation trees. We have conducted experiments on our new SRSD datasets using five state-of-the-art SR methods in SRBench and a simple baseline based on a recent Transformer architecture. The results show that we provide a more realistic performance evaluation and open up a new machine learning-based approach for scientific discovery. Our datasets^{1 2 3} and code repository⁴ are publicly available.

1 Introduction

Recent advances in machine learning (ML), especially deep learning (DL), have led to the proposal of many methods that can reproduce the given data and make appropriate inferences on new inputs. Such methods are, however, often black-box, which makes it difficult for humans to understand how they made predictions for given inputs. This property will be more critical especially when non-ML experts apply ML to problems in their research domains such as physics and chemistry.

Symbolic regression (SR) is the task of producing a mathematical expression (symbolic expression) that fits a given dataset. SR has been studied in the genetic programming (GP) community [14, 17, 19,

*This work was mainly done while the first author was a research intern at OMRON SINIC X Corporation.

¹https://huggingface.co/datasets/yoshitomo-matsubara/srsd-feynman_easy

²https://huggingface.co/datasets/yoshitomo-matsubara/srsd-feynman_medium

³https://huggingface.co/datasets/yoshitomo-matsubara/srsd-feynman_hard

⁴<https://github.com/omron-sinicx/srsd-benchmark>

22, 38, 50], and DL-based SR has been attracting more attention from the ML/DL community [4, 18, 26, 27, 40, 51]. Because of its interpretability, various scientific communities apply SR to advance research in their scientific fields *e.g.*, Physics [7, 20, 30, 31, 48, 49, 59], Applied Mechanics [15], Climatology [1], Materials [32, 46, 55, 57], and Chemistry [3].

Given that SR has been studied in various communities, La Cava et al. [26] propose SRBench, a unified benchmark framework for symbolic regression methods. In the benchmark study, they combine the Feynman Symbolic Regression Database (FSRD) [48] and the ODE-Strogatz repository [45] to compare a number of SR methods, using a large-scale heterogeneous computing cluster.⁵

To discuss the potential of symbolic regression for scientific discovery (SRSD), there still remain some issues to be addressed: oversimplified datasets and lack of evaluation metric towards SRSD. For symbolic regression tasks, existing datasets consist of values sampled from limited domains such as in range of 1 to 5, and there are no large-scale datasets with reasonably realistic values that capture the properties of the formula and its variables. Thus, it is difficult to discuss the potential of symbolic regression for scientific discovery with such existing datasets. For instance, the FSRD consists of 120 formulas selected mostly from Feynman Lectures Series⁶ [10–12] and are core benchmark datasets used in SRBench [26]. While the formulas indicate physical laws, variables and constants used in each dataset have no physical meanings since the datasets are not designed to discover the physical laws from the observed data in the real world. (See Section 3.1.)

Moreover, there is a lack of appropriate metrics to evaluate these methods for SRSD. An intuitive approach would be to measure the prediction error or correlation between the predicted values and the target values in the test data, as in standard regression problems. However, low prediction errors could be achieved even by complex models that differ from the original law. In addition, SRBench [26] present the percentage of agreement between the target and the estimated equations. But in such cases, both 1) equations that do not match at all and 2) that differ by only one term⁷ are equally treated as incorrect. As a result, it is considered as a coarse-resolution evaluation method for accuracy in SRSD, which still needs more discussion towards real-world applications. A key feature of SR is its interpretability, and some studies [26, 49] use complexity of the predicted expression as an evaluation metric (the simpler the better). However, it is based on a big assumption that a simpler expression may be more likely to be a hidden law in the data (scientific discovery such as physics law), which may not be true for SRSD. Therefore, there are no single evaluation metrics proposed to take into account both the interpretability and how close to the true expression the estimated expression is.

To address these issues, we propose new SRSD datasets, introduce a new evaluation method, and conduct benchmark experiments using representative SR methods and a new Transformer-based SR baseline. We carefully review and design annotation policies for the new datasets, considering the properties of the physics formulas. Besides, given that a formula can be represented as a tree structure, we introduce a normalized edit distance on the tree structure to allow quantitative evaluation of predicted formulas that do not perfectly match the true formulas. Using the proposed SRSD datasets and evaluation metric, we perform benchmark experiments with a set of SR baselines and find that there is still significant room for improvements in terms of the new evaluation metric.

2 Related Studies

In this section, we briefly introduce related studies focused on 1) symbolic regression for scientific discovery and 2) symbolic regression dataset and evaluation.

2.1 SRSD: Symbolic Regression for Scientific Discovery

A pioneer study on symbolic regression for scientific discovery is conducted by Schmidt & Lipson [42], who propose a data-driven scientific discovery method. They collect data from standard experimental systems like those used in undergrad physics education: an air-track oscillator and a double pendulum. Their proposed algorithm detects different types of laws from the data such as position manifolds, energy laws, and equations of motion and sum of forces laws.

⁵They used hosts with 24–28 core Intel(R) Xeon(R) CPU E5-2690 v4 2.60GHz processors and 250GB RAM.

⁶Udrescu & Tegmark [48] extract 20 of the 120 equations as “bonus” from other seminal books [13, 16, 44, 56].

⁷If those differ by a constant or scalar, SRBench treats the estimated equation as correct.

Following the study, data-driven scientific discovery has been attracting attention from research communities and been applied to various domains such as Physics [7, 20, 30, 31, 48, 49, 59], Applied Mechanics [15], Climatology [1], Materials [32, 46, 55, 57], and Chemistry [3].

These studies leverage symbolic regression in different fields. While general symbolic regression tasks use synthetic datasets with limited sampling domains for benchmarks, many of the SRSD studies collect data from the real world and discuss how we could leverage symbolic regression toward scientific discovery.

While SRSD tasks share the same input-output interface with general symbolic regression (SR) tasks (*i.e.*, input: dataset, output: symbolic expression), we differentiate SRSD tasks in this study from general SR tasks by whether or not the datasets including true symbolic expressions are created with reasonably realistic assumptions for scientific discovery such as meaning of true symbolic expressions (whether or not they have physical meanings) and sampling domains for input variables.

2.2 Dataset and Evaluation

For symbolic regression methods, there exist several benchmark datasets and empirical studies. The Feynman Symbolic Regression Database [48] is one of the largest symbolic regression datasets, which consists of 100 physics-inspired equations based on Feynman Lectures on Physics [10–12]. By randomly sampling from small ranges of value, they generate the corresponding tabular datasets for the 100 equations. Inspired by [14, 17, 19], Uy et al. [50] suggest 10 different real-valued symbolic regression problems (functions) and create the corresponding dataset (*a.k.a.* Nguyen dataset). The suggested functions consist of either 1 or 2 variables *e.g.*, $f(x) = x^6 + x^5 + x^4 + x^3 + x^2 + x$ and $f(x, y) = \sin(x) + \sin(y^2)$. They generate each dataset by randomly sampling 20 - 100 data points.

La Cava et al. [26] design a symbolic regression benchmark, named SRBench, and conduct a comprehensive benchmark experiment, using existing symbolic regression datasets such as the Feynman Symbolic Regression Database [48] and ODE-Strogatz repository [23]. In SRBench, symbolic regression methods are assessed by 1) an error metric based on squared error between target and estimated values, and 2) solution rate that shows a percentage of the estimated symbolic regression models that match the true models (equations).

However, these datasets and evaluations are not necessarily designed to discuss symbolic regression for scientific discovery. In Sections 3.1 and 4.1, we further describe potential issues in prior studies.

3 Datasets

In this section, we summarize issues we found in the existing symbolic regression datasets, and then propose new datasets to address them towards symbolic regression for scientific discovery (SRSD).

3.1 Issues in Existing Datasets

As introduced in Section 2.2, there are many symbolic regression datasets. However, we consider that novel datasets are required to discuss SRSD for the following reasons:

1. **No physical meaning:** Many of the existing symbolic regression datasets [14, 17, 19, 50] are not necessarily physics-inspired, but instead randomly generated *e.g.*, $f(x) = \log(x)$, $f(x, y) = xy + \sin((x - 1)(y - 1))$. To discuss the potential of symbolic regression for scientific discovery, we need to further elaborate datasets and evaluation metrics, considering how we would leverage symbolic regression in practice.
2. **Oversimplified sampling process:** While some of the datasets are physics-inspired such as the Feynman Symbolic Regression Database (FSRD) [48] and ODE-Strogatz repository [23], their sampling strategies are very simplified. Specifically, the strategies do not distinguish between constants and variables *e.g.*, speed of light⁸ is treated as a variable and randomly sampled in range of 1 to 5. Besides, most of the sampling domains are far from values we could observe in the real world *e.g.*, II.4.23 in Table S1 (the vacuum permittivity values are sampled from range of 1 to 5). When sampled ranges of the distributions are narrow, we cannot

⁸We treat speed of light as a constant (2.998×10^8 m/s) in this study.

distinguish Lorentz transformation from Galilean transformation *e.g.* I.15.10 and I.16.6 in Table S3, I.48.2 in Table S5, I.15.3t, I.15.3x, and I.34.14 in Table S7, or the black body radiation can be misestimated to Stephan-Boltzmann law or the Wien displacement law *e.g.* I.41.16 in Table S8.

3. **Duplicate equations:** Due to the two issues above, many of the equations in existing datasets turn out to be duplicate. *e.g.*, as shown in Table 1, $F = \mu N_n$ (I.12.1) and $F = q_2 E$ (I.12.5) in the *original* Feynman Symbolic Regression Database are considered identical since both the equations are multiplicative and consists of two variables, and their sampling domains (Distributions in Table 1) are exactly the same. For instance, approximately 25% of the symbolic regression problems in the *original* FSRD have 1 - 5 duplicates in that regard.
4. **Incorrect/Inappropriate formulas:** The Feynman Symbolic Regression Database [48] treat every variables as float whereas they should be integer to be physically meaningful. For example, the number of phase difference in Bragg's law should be integer but sampled as real number (I.30.5 in Table S1). Furthermore, they don't even give special treatment of angle variables (I.18.12, I.18.16, and I.26.2 in Table 1). Physically some variables can be negative whereas the *original* Feynman Symbolic Regression Database [48] only samples positive values (*e.g.* I.8.14 and I.11.19 in Table S3). We also avoid using \arcsin/\arccos in the equations since the use of \arcsin/\arccos in the Feynman Symbolic Regression Database [48] just to obtain angle variable is not experimentally meaningful (I.26.2 in Table 1, I.30.5 in Table S1, and B10 in Table S11). Equations using \arcsin and \arccos in the original annotation are I.26.2 (Snell's law), I.30.5 (Bragg's law), and B10 (Relativistic aberration). These are all describing physical phenomena related to two angles, and it is an unnatural deformation to describe only one of them with an inverse function. Additionally, inverse function use implicitly limits the range of angles, but there is no such limitation in the actual physical phenomena.

3.2 Proposed SRSD Datasets

We address the issues in existing datasets above by proposing new SRSD datasets based on the equations used in the FSRD [48]. *i.e.*, Section 3.1 summarizes the differences between the FSRD and our SRSD datasets. Our annotation policy is carefully designed to simulate typical physics experiments so that the SRSD datasets can engage studies on symbolic regression for scientific discovery in the research community.

3.2.1 Annotation policy

We thoroughly revised the sampling range for each variable from the annotations in the FSRD [48]. First, we reviewed the properties of each variable and treated physical constants (*e.g.*, light speed, gravitational constant) as constants while such constants are treated as variables in the original FSRD datasets. Next, variable ranges were defined to correspond to each typical physics experiment to confirm the physical phenomenon for each equation. We also used [36] as a reference. In cases where a specific experiment is difficult to be assumed, ranges were set within which the corresponding physical phenomenon can be seen. Generally, the ranges are set to be sampled on log scales within their orders as 10^2 in order to take both large and small changes in value as the order changes. Variables such as angles, for which a linear distribution is expected are set to be sampled uniformly. In addition, variables that take a specific sign were set to be sampled within that range. Tables 1 and S1 – S11 show the detailed comparisons between the original FSRD and our proposed SRSD datasets.

3.2.2 Complexity-aware Dataset Categories

While the proposed datasets consist of 120 different problems, there will be non-trivial training cost required to train a symbolic regression model for all the problems individually [26] *i.e.*, there will be 120 separate training sessions to assess the symbolic regression approach. To allow more flexibility in assessing symbolic regression models for scientific discovery, we define three clusters of the proposed datasets based on their complexity: *Easy*, *Medium*, and *Hard* sets, which consist of 30, 40, and 50 different problems respectively.

We define the complexity of problem, using the number of operations to represent the true equation tree and range of the sampling domains. The former measures how many mathematical operations

Table 1: Easy set of our proposed datasets (part 1). C: Constant, V: Variable, F: Float, I: Integer, P: Positive, N: Negative, NN: Non-Negative, \mathcal{U} : Uniform distribution, \mathcal{U}_{\log} : Log-Uniform distribution.

Eq. ID	Formula	Symbols	Properties		Distributions	
			Original	Ours	Original	Ours
I.12.1	$F = \mu N_n$	F	Force of friction	V, F	V, F, P	N/A
		μ	Coefficient of friction	V, F	V, F, P	$\mathcal{U}(1, 5)$ $\mathcal{U}_{\log}(10^{-2}, 10^0)$
		N_n	Normal force	V, F	V, F, P	$\mathcal{U}(1, 5)$ $\mathcal{U}_{\log}(10^{-2}, 10^0)$
I.12.4	$E = \frac{q_1}{4\pi\epsilon r^2}$	E	Magnitude of electric field	V, F	V, F	N/A
		q_1	Electric charge	V, F	V, F	$\mathcal{U}(1, 5)$ $\mathcal{U}_{\log}(10^{-3}, 10^{-1})$
		r	Distance	V, F	V, F, P	$\mathcal{U}(1, 5)$ $\mathcal{U}_{\log}(10^{-2}, 10^0)$
		ϵ	Vacuum permittivity	V, F	C, F, P	$\mathcal{U}(1, 5)$ 8.854×10^{-12}
I.12.5	$F = q_2 E$	F	Force	V, F	V, F	N/A
		q_2	Electric charge	V, F	V, F	$\mathcal{U}(1, 5)$ $\mathcal{U}_{\log}(10^{-3}, 10^{-1})$
		E	Electric field	V, F	V, F	$\mathcal{U}(1, 5)$ $\mathcal{U}_{\log}(10^1, 10^3)$
I.14.3	$U = mgz$	U	Potential energy	V, F	V, F, P	N/A
		m	Mass	V, F	V, F, P	$\mathcal{U}(1, 5)$ $\mathcal{U}_{\log}(10^{-2}, 10^0)$
		g	Gravitational acceleration	V, F	C, F, P	$\mathcal{U}(1, 5)$ 9.807×10^0
		z	Height	V, F	V, F	$\mathcal{U}(1, 5)$ $\mathcal{U}_{\log}(10^{-2}, 10^0)$
I.14.4	$U = \frac{k_{\text{spring}}x^2}{2}$	U	Elastic energy	V, F	V, F, P	N/A
		k_{spring}	Spring constant	V, F	V, F, P	$\mathcal{U}(1, 5)$ $\mathcal{U}_{\log}(10^2, 10^4)$
		x	Position	V, F	V, F	$\mathcal{U}(1, 5)$ $\mathcal{U}_{\log}(10^{-2}, 10^0)$
I.18.12	$\tau = rF \sin \theta$	τ	Torque	V, F	V, F	N/A
		r	Distance	V, F	V, F, P	$\mathcal{U}(1, 5)$ $\mathcal{U}_{\log}(10^{-1}, 10^1)$
		F	Force	V, F	V, F	$\mathcal{U}(1, 5)$ $\mathcal{U}_{\log}(10^{-1}, 10^1)$
		θ	Angle	V, F	V, F, NN	$\mathcal{U}(0, 5)$ $\mathcal{U}(0, 2\pi)$
I.18.16	$L = mr v \sin \theta$	L	Angular momentum	V, F	V, F	N/A
		m	Mass	V, F	V, F, P	$\mathcal{U}(1, 5)$ $\mathcal{U}_{\log}(10^{-1}, 10^1)$
		r	Distance	V, F	V, F, P	$\mathcal{U}(1, 5)$ $\mathcal{U}_{\log}(10^{-1}, 10^1)$
		v	Velocity	V, F	V, F, P	$\mathcal{U}(1, 5)$ $\mathcal{U}_{\log}(10^{-1}, 10^1)$
I.25.13	$V = \frac{q}{C}$	θ	Angle	V, F	V, F, NN	$\mathcal{U}(1, 5)$ $\mathcal{U}(0, 2\pi)$
		V	Voltage	V, F	V, F	N/A
		q	Electric charge	V, F	V, F	$\mathcal{U}(1, 5)$ $\mathcal{U}_{\log}(10^{-5}, 10^{-3})$
I.26.2	$n = \frac{\sin \theta_1}{\sin \theta_2}$	C	Electrostatic Capacitance	V, F	V, F, P	$\mathcal{U}(1, 5)$ $\mathcal{U}_{\log}(10^{-5}, 10^{-3})$
		n	Relative refractive index	V, F	V, F, P	$\mathcal{U}(0, 1)$ N/A
		θ_1	Refraction angle 1	V, F	V, F	N/A
I.27.6	$f = \frac{1}{\frac{1}{d_1} + \frac{n}{d_2}}$	θ_2	Refraction angle 2	V, F	V, F	$\mathcal{U}(1, 5)$ $\mathcal{U}(0, \frac{\pi}{2})$
		f	Focal length	V, F	V, F	N/A
		d_1	Distance	V, F	V, F, P	$\mathcal{U}(1, 5)$ $\mathcal{U}_{\log}(10^{-3}, 10^{-1})$
		n	Refractive index	V, F	V, F, P	$\mathcal{U}(1, 5)$ $\mathcal{U}_{\log}(10^{-1}, 10^1)$
		d_2	Distance	V, F	V, F, P	$\mathcal{U}(1, 5)$ $\mathcal{U}_{\log}(10^{-3}, 10^{-1})$

compose the true equation such as *add*, *mul*, *pow*, *exp*, and *log* operations (see Fig. 2). The latter considers magnitude of sampling distributions (*Distributions* column in Tables 1 and S1 – S11) and increases the complexity when sampling values from wide range of distributions. We define the domain range as follows:

$$f_{\text{range}}(\mathcal{S}) = \left| \log_{10} \left| \max_{s \in \mathcal{S}} s - \min_{s \in \mathcal{S}} s \right| \right|, \quad (1)$$

where \mathcal{S} indicates a set of sampling domains (*distributions*) for a given symbolic regression problem.

As we will show in Section 5.3, these clusters represent problem difficulties at high level. For instance, these subsets will help the research community to shortly tune and/or perform sanity-check new approaches on the *Easy* set (30 problems) instead of using the whole datasets (120 problems). Figure 1 shows the three different distribution maps of our proposed datasets. *Easy*, *Medium*, and *Hard* sets consist of 30, 40, and 50 individual symbolic regression problems, respectively.

4 Benchmark

Besides the conventional metrics, we propose a new metric to discuss the performance of symbolic regression for scientific discovery in Section 4.1. Following the set of metrics, we design an evaluation framework of symbolic regression for scientific discovery.

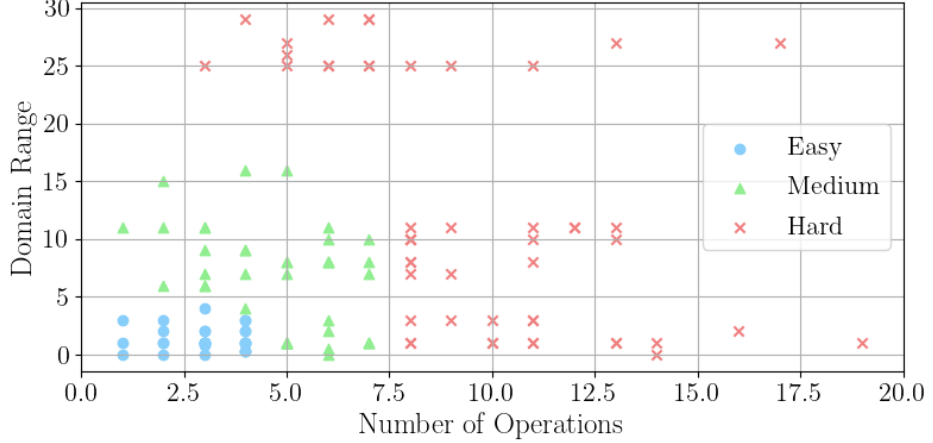


Figure 1: Distribution map of our proposed datasets based on three different subsets with respect to our complexity metrics. Data points at top right/bottom left indicate more/less complex problems.

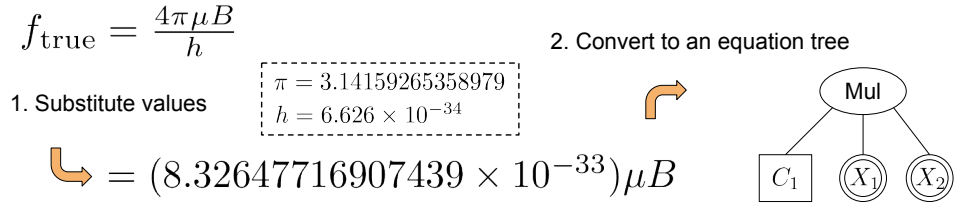


Figure 2: Example of preprocessing a true equation (III.7.38 in Table S1) in evaluation session. When converting to an equation tree, we replace constant values and variables with specific symbols *e.g.*, $8.32647716907439 \times 10^{-33} \rightarrow C_1, \mu \rightarrow X_1, B \rightarrow X_2$.

4.1 Metrics

In general, it would be difficult to define “accuracy” of symbolic regression models since we will compare its estimated equation to the ground truth equation and need criteria to determine whether or not it is “correct”. La Cava et al. [26] suggested a reasonable definition of symbolic solution, which is designed to capture symbolic regression models that differ from the true model by a constant or scalar. They also used R^2 score (Eq. 2) and define as accuracy the percentage of symbolic regression problems that a model meets $R^2 > \tau$, where τ is a threshold *e.g.*, $\tau = 0.999$ in [26].

$$R^2 = \frac{\sum_j^N (f_{\text{pred}}(X_j) - f_{\text{true}}(X_j))^2}{\sum_k^N (f_{\text{true}}(X_k) - \bar{y})^2}, \quad (2)$$

where N indicates the number of test samples (*i.e.*, the number of rows in the test dataset), and \bar{y} is a mean of target outputs produced by f_{true} . f_{pred} and f_{true} are a trained SR model and a true model, respectively. However, these two metrics are still binary (correct or not) or require a threshold and does not explain how *structurally close* to the true equation the estimated one is. While a key feature of symbolic regression is its interpretability, there are no single evaluation metrics to take into account both the interpretability and how close to the true expression the estimated expression is.

To offer more flexibility and assess estimated equations in such a way, we propose the use of edit distance between estimated and ground truth equations, processing equations as trees. Although edit distance has been employed in different domains such as machine translation [41] (text-based edit distance), its primary use has been to study the search process for genetic programming approaches [5, 35, 37]. Different from prior work, we propose a use of tree-based edit distance as a new metric of solution quality for SRSD.

For a pair of two trees, edit distance computes the minimum cost to transform one to another with a sequence of operations, each of which either 1) *inserts*, 2) *deletes*, or 3) *renames* a node. In this study, a node can be either a mathematical operation (e.g., *add*, *exp* as symbols), a variable symbol, or a constant symbol. For the detail of the algorithm, we refer readers to [61].

As illustrated in Fig. 2, we preprocess equations by 1) substituting constant values e.g., π and Planck constant to the expression, and 2) converting the resulting expression to an equation tree that represents the preorder traversal of the equation with simplified symbols. It should be worth noting that before generating the equation tree, we simplify and convert equations to floating-point approximations by `sympy` [34], a Python library for symbolic mathematics. It helps us consistently map a given equation to the unique equation tree and compute edit distance between the true and estimated equation trees since our evaluation interest is in simplified expressions of the estimated equations rather than how SR models produced the equations. For instance, “ $x + x + x$ ”, “ $4 * x - x$ ”, and “ $x + 2 * x$ ” will be simplified by `sympy` to “ $3 * x$ ” and considered identical.

For edit distance, we use a method proposed by Zhang & Shasha [61]. Given that the range of edit distance values depends on complexity of equations, we normalize the distance in range of 0 to 1 as

$$\bar{d}(f_{\text{pred}}, f_{\text{true}}) = \min \left(1, \frac{d(f_{\text{pred}}, f_{\text{true}})}{|f_{\text{true}}|} \right), \quad (3)$$

where f_{pred} and f_{true} are estimated and true equation trees, respectively. $d(f_{\text{pred}}, f_{\text{true}})$ is an edit distance between f_{pred} and f_{true} . $|f_{\text{true}}|$ indicates the number of the tree nodes that compose an equation f_{true} . We note that this metric is designed to capture similarity between estimated and true equations, thus coefficient values themselves (e.g., value of C_1 in Fig. 2) should not be important.

4.2 Evaluation Framework

For real datasets (assuming observed datasets), only tabular data are available for training and validation. (In practice, a test dataset does not include the true equation.) For benchmark purposes, true equations are provided as test data besides test tabular data.

For each problem, we use the validation tabular dataset and choose the best trained SR model f_{pred}^* from \mathcal{F} , a set of the trained models by a given method respect to Eq. (4)

$$f_{\text{pred}}^* = \arg \min_{f_{\text{pred}} \in \mathcal{F}} \frac{1}{n} \sum_{i=1}^n \left| \frac{f_{\text{pred}}(X_i) - f_{\text{true}}(X_i)}{f_{\text{true}}(X_i)} \right|^2, \quad (4)$$

where X_i indicates the i -th row of the validation tabular dataset X .

Notice that while we proposed in Section 4.1 a normalized edit distance between estimated and true equation trees, such true equations will not be available in practice, especially when using symbolic regression methods for scientific discovery. For this reason, we use the geometrical distance between predicted values against a validation tabular dataset to choose the best model obtained through hyperparameter tuning. Using the best model per method, we compute the normalized edit distance to assess the method.

5 Experiments

5.1 Baseline Methods

For baselines, we use the five best symbolic regression methods in SRBench [26]. Specifically, we choose gplearn [22], AFP [43], AFP-FE [42], AI Feynman [49], and DSR [40], referring to the rankings of solution rate for the FSRD datasets in their study. We note that La Cava et al. [26] also benchmark symbolic regression methods for black-box problems, whose true symbolic expressions are unknown, and other symbolic regression methods e.g., Operon [21], SBP-GP [53], FEAT [24], EPLEX [25], and GP-GOMEA [54] outperform the five baseline methods we choose from their study, in terms of R^2 -driven accuracy. However, we find solution rate more aligned with edit distance, thus we choose the five best symbolic regression methods in terms of solution rate empirically shown for the FSRD datasets in SRBench [26]. In addition to the five existing symbolic regression baselines, we introduce Symbolic Transformer, a new baseline model with Transformer [52]:

1. **gplearn** [22]: a genetic programming based symbolic regression method published as a Python package gplearn.
2. **AFP** [43]: Age-fitness pareto optimization.
3. **AFP-FE** [42]: AFP optimization with fitness estimates.
4. **AI Feynman** [49]: an iterative approach to generate symbolic regression to seek to fit data to formulas that are Pareto-optimal.
5. **DSR** [40]: reinforcement learning based deep symbolic regression.
6. **Symbolic Transformer (ST)**: our Transformer-based symbolic regression baseline.

For the details of the baseline models, we refer readers to the corresponding papers [22, 40, 42, 43, 49]. We provide the details of Symbolic Transformer in Section C, including our pretraining strategy. While Symbolic Transformer itself is a new model, we note that the main contribution of this work lies in the datasets and benchmark of symbolic regression for scientific discovery. Our Transformer-based baseline method is simply inspired by recent advances in deep learning, specifically transformer-based high-performance, modern, and flexible models such as [8, 9, 52]. Thus, the new model is not necessarily designed to show improvements over the existing Transformer-based symbolic regression models [4, 51] including contemporary work such as [18].

5.2 Runtime Constraints

The implementations of the baseline methods in Section 5.1 except Symbolic Transformer⁹ do not use any GPUs. We run 600 high performance computing (HPC) jobs in total, using “C.small” and “C.large” computing nodes, which have 5 - 20 assigned physical CPU cores, 30 - 120 GB RAM, and 720 GB local storage available in AI Bridging Cloud Infrastructure (ABCI).¹⁰ Due to the properties of our HPC resource, we have some runtime constraints:

1. Since each HPC job is designed to run for up to 24 hours due to the limited resource, we run a job with a pair of a target tabular dataset and a symbolic regression method.
2. Given a pair of a dataset and a method, each of our HPC jobs runs up to 100 separate training sessions with different hyperparameter values.

5.3 Results

In this section, we discuss the experimental results of our baseline methods, using the proposed SRSD datasets. Tables 2 and 3 show the performance of the symbolic regression baseline methods in terms of R^2 -driven accuracy ($R^2 > 0.999$) and solution rate respectively, and both the metrics are used in SRBench [26]. According to the metrics, DSR significantly outperforms all the other baselines we considered. The DSR results also indicate difficulty levels of the three categories of our SRSD datasets, which looks aligned with our complexity-aware dataset categorization (Section 3.2.2).

Now we discuss the results using the normalized edit distance. Table 4 show the results of the baseline methods in terms of the normalized edit distance. Interestingly, while the Symbolic Transformer performed the worst in Table 2 in terms of R^2 -based accuracy, it achieved the best normalized edit distance for all the SRSD Easy, Medium, and Hard sets and significantly improved DSR. This trend also implies that the R^2 -based accuracy does not always indicate how well the SR model can produce an equation that is *structurally close* to the true equation. We also confirmed that the difficulty level of each set of SRSD datasets is reflected to the overall trend in Tables 2 - 4.

6 Limitations

6.1 Implicit Functions

Symbolic regression generally has a limitation in inferring implicit functions, as the model infers a trivial constant function if there are no restrictions on variables. For example, $f(x, y) = 0$ is inferred

⁹We used an NVIDIA GeForce RTX 3070 Ti for pretraining Symbolic Transformer.

¹⁰https://abci.ai/en/how_to_use/tariffs.html

Table 2: Baseline results: accuracy ($R^2 > 0.999$) defined by La Cava et al. [26].

SRSD Datasets \ Method	gplearn	AFP	AFP-FE	AI Feynman	DSR	ST
Easy set (30 problems)	6.67%	20.0%	23.3%	33.3%	60.0%	0.00%
Medium set (40 problems)	7.50%	2.50%	2.50%	5.00%	42.5%	0.00%
Hard set (50 problems)	2.00%	4.00%	4.00%	8.00%	30.0%	0.00%

Table 3: Baseline results: solution rate defined by La Cava et al. [26].

SRSD Datasets \ Method	gplearn	AFP	AFP-FE	AI Feynman	DSR	ST
Easy set (30 problems)	6.67%	20.0%	20.0%	30.0%	43.3%	16.7%
Medium set (40 problems)	2.50%	2.50%	2.50%	2.50%	10.0%	5.00%
Hard set (50 problems)	0.00%	0.00%	0.00%	2.00%	2.00%	0.00%

Table 4: Baseline results: our proposed normalized edit distances (the smaller the better).

SRSD Datasets \ Method	gplearn	AFP	AFP-FE	AI Feynman	DSR	ST
Easy set (30 problems)	0.876	0.703	0.712	0.646	0.551	0.435
Medium set (40 problems)	0.939	0.873	0.897	0.936	0.789	0.556
Hard set (50 problems)	0.978	0.960	0.956	0.930	0.833	0.704

as $0 = 0 \forall x, y$. This problem can be solved by applying the constraint that an inferred function should depend on at least two variables *e.g.*, inferring $f(x, y) = 0$ with $\frac{\partial f}{\partial x} \neq 0$ and $\frac{\partial f}{\partial y} \neq 0$, or by converting the function to an explicit form *e.g.*, $y = g(x)$. We converted some functions in the datasets into explicit forms and avoided the inverse trigonometric functions as described in Section 3.1.

6.2 Dummy Variables and Noise Injection

When applying machine learning to real-world problems, it is often true that 1) not all the observed features (variables in symbolic regression) are necessary to solve the problems, and 2) the observed values contain some noise. While we follow [26] and show experimental results for our SRSD datasets with noise-injected target variables in Section E, these aspects are not thoroughly discussed in this study, such discussions can be a separate paper built on this work and further engage studies of symbolic regression for scientific discovery.

7 Conclusion

In this work, we pointed out issues of existing datasets and benchmarks of symbolic regression for scientific discovery (SRSD). To address the issues, we proposed 1) 120 new SRSD datasets based on a set of physics formulas in FSRD [48] and 2) a new evaluation metric for SRSD to discuss the structural similarity between the true and estimated symbolic expressions (equations). We note that this study argues that the normalized edit distance is a metric not to take the place of existing SR metrics but to incorporate such metrics (*e.g.*, Tables 2 and 4). Besides the main contribution above, we proposed a Transformer-based symbolic regression baseline, named Symbolic Transformer that achieved the best normalized edit distance for the proposed SRSD datasets. To encourage the studies of SRSD, we publish our datasets^{1,2,3} and code repository⁴ with MIT License.

Acknowledgments

In this study, we used the computing resource of AI Bridging Cloud Infrastructure (ABCi) provided by National Institute of Advanced Industrial Science and Technology (AIST). This work is supported by JST-Mirai Program Grant Number JPMJMI21G2, Japan.

References

- [1] Ismail Alaoui Abdellaoui and Siamak Mehrkanoon. Symbolic regression for scientific discovery: an application to wind speed forecasting. In *2021 IEEE Symposium Series on Computational Intelligence (SSCI)*, pp. 01–08. IEEE, 2021.
- [2] Takuya Akiba, Shotaro Sano, Toshihiko Yanase, Takeru Ohta, and Masanori Koyama. Optuna: A Next-generation Hyperparameter Optimization Framework. In *Proceedings of the 25th ACM SIGKDD international conference on knowledge discovery & data mining*, pp. 2623–2631, 2019.
- [3] Rohit Batra, Le Song, and Rampi Ramprasad. Emerging materials intelligence ecosystems propelled by machine learning. *Nature Reviews Materials*, pp. 1–24, 2020.
- [4] Luca Biggio, Tommaso Bendinelli, Alexander Neitz, Aurelien Lucchi, and Giambattista Pascaniolo. Neural Symbolic Regression that Scales. In *International Conference on Machine Learning*, pp. 936–945. PMLR, 2021.
- [5] Edmund Burke, Steven Gustafson, Graham Kendall, and Natalio Krasnogor. Advanced Population Diversity Measures in Genetic Programming. In *International Conference on Parallel Problem Solving from Nature*, pp. 341–350. Springer, 2002.
- [6] R. Qi Charles, Hao Su, Mo Kaichun, and Leonidas J. Guibas. Pointnet: Deep learning on point sets for 3d classification and segmentation. In *IEEE/CVF Conference on Computer Vision and Pattern Recognition (CVPR)*, 2017.
- [7] Miles Cranmer, Alvaro Sanchez Gonzalez, Peter Battaglia, Rui Xu, Kyle Cranmer, David Spergel, and Shirley Ho. Discovering Symbolic Models from Deep Learning with Inductive Biases. *Advances in Neural Information Processing Systems*, 33:17429–17442, 2020.
- [8] Jacob Devlin, Ming-Wei Chang, Kenton Lee, and Kristina Toutanova. BERT: Pre-training of Deep Bidirectional Transformers for Language Understanding. In *Proceedings of the 2019 Conference of the North American Chapter of the Association for Computational Linguistics: Human Language Technologies, Volume 1 (Long and Short Papers)*, pp. 4171–4186, 2019.
- [9] Alexey Dosovitskiy, Lucas Beyer, Alexander Kolesnikov, Dirk Weissenborn, Xiaohua Zhai, Thomas Unterthiner, Mostafa Dehghani, Matthias Minderer, Georg Heigold, Sylvain Gelly, et al. An Image is Worth 16x16 Words: Transformers for Image Recognition at Scale. In *International Conference on Learning Representations*, 2020.
- [10] Richard P Feynman, Robert B Leighton, and Matthew Sands. *The Feynman Lectures on Physics, Vol. I: The New Millennium Edition: Mainly Mechanics, Radiation, and Heat*, volume 1. Basic books, 1963.
- [11] Richard P Feynman, Robert B Leighton, and Matthew Sands. *The Feynman Lectures on Physics, Vol. II: The New Millennium Edition: Mainly Electromagnetism and Matter*, volume 2. Basic books, 1963.
- [12] Richard P Feynman, Robert B Leighton, and Matthew Sands. *The Feynman Lectures on Physics, Vol. II: The New Millennium Edition: Quantum Mechanics*, volume 3. Basic books, 1963.
- [13] Herbert Goldstein, Charles Poole, and John Safko. *Classical Mechanics*. Addison Wesley, 2002.
- [14] Nguyen Xuan Hoai, Robert Ian McKay, D Essam, and R Chau. Solving the Symbolic Regression Problem with Tree Adjunct Grammar Guided Genetic Programming: The Comparative Results. In *Proceedings of the 2002 Congress on Evolutionary Computation. CEC'02 (Cat. No. 02TH8600)*, volume 2, pp. 1326–1331. IEEE, 2002.
- [15] Zhanchao Huang, Chunjiang Li, Zhilong Huang, Yong Wang, and Hanqing Jiang. AI-Timoshenko: Automatedly Discovering Simplified Governing Equations for Applied Mechanics Problems From Simulated Data. *Journal of Applied Mechanics*, 88(10):101006, 2021.
- [16] John David Jackson. *Classical Electrodynamics*. Wiley, 1999.

[17] Colin G Johnson. Genetic Programming Crossover: Does it Cross Over? In *European Conference on Genetic Programming*, pp. 97–108. Springer, 2009.

[18] Pierre-Alexandre Kamienny, Stéphane d’Ascoli, Guillaume Lample, and François Charton. End-to-end symbolic regression with transformers. *arXiv preprint arXiv:2204.10532*, 2022.

[19] Maarten Keijzer. Improving Symbolic Regression with Interval Arithmetic and Linear Scaling. In *European Conference on Genetic Programming*, pp. 70–82. Springer, 2003.

[20] Samuel Kim, Peter Y Lu, Srijon Mukherjee, Michael Gilbert, Li Jing, Vladimir Čepelić, and Marin Soljačić. Integration of Neural Network-Based Symbolic Regression in Deep Learning for Scientific Discovery. *IEEE Transactions on Neural Networks and Learning Systems*, 2020.

[21] Michael Kommenda, Bogdan Burlacu, Gabriel Kronberger, and Michael Affenzeller. Parameter identification for symbolic regression using nonlinear least squares. *Genetic Programming and Evolvable Machines*, 21(3):471–501, 2020.

[22] John R Koza and Riccardo Poli. Genetic Programming. In *Search methodologies*, pp. 127–164. Springer, 2005.

[23] William La Cava, Kourosh Danai, and Lee Spector. Inference of compact nonlinear dynamic models by epigenetic local search. *Engineering Applications of Artificial Intelligence*, 55: 292–306, 2016.

[24] William La Cava, Tilak Raj Singh, James Taggart, Srinivas Suri, and Jason H Moore. Learning concise representations for regression by evolving networks of trees. In *International Conference on Learning Representations*, 2018.

[25] William La Cava, Thomas Helmuth, Lee Spector, and Jason H Moore. A Probabilistic and Multi-Objective Analysis of Lexicase Selection and ε -Lexicase Selection. *Evolutionary Computation*, 27(3):377–402, 2019.

[26] William La Cava, Patryk Orzechowski, Bogdan Burlacu, Fabricio Olivetti de Franca, Marco Virgolin, Ying Jin, Michael Kommenda, and Jason H Moore. Contemporary Symbolic Regression Methods and their Relative Performance. In *Thirty-fifth Conference on Neural Information Processing Systems Datasets and Benchmarks Track (Round 1)*, 2021.

[27] Mikel Landajuela, Brenden K Petersen, Sookyung Kim, Claudio P Santiago, Ruben Glatt, Nathan Mundhenk, Jacob F Pettit, and Daniel Faissol. Discovering symbolic policies with deep reinforcement learning. In *International Conference on Machine Learning*, pp. 5979–5989. PMLR, 2021.

[28] Yijin Liu, Fandong Meng, Yufeng Chen, Jinan Xu, and Jie Zhou. Scheduled Sampling Based on Decoding Steps for Neural Machine Translation. In *Proceedings of the 2021 Conference on Empirical Methods in Natural Language Processing*, pp. 3285–3296, 2021.

[29] Yinhan Liu, Myle Ott, Naman Goyal, Jingfei Du, Mandar Joshi, Danqi Chen, Omer Levy, Mike Lewis, Luke Zettlemoyer, and Veselin Stoyanov. RoBERTa: A Robustly Optimized BERT Pretraining Approach. *arXiv preprint arXiv:1907.11692*, 2019.

[30] Z Liu, B Wang, Q Meng, W Chen, M Tegmark, and TY Liu. Machine-learning nonconservative dynamics for new-physics detection. *Physical Review E*, 104(5-2):055302–055302, 2021.

[31] Ziming Liu and Max Tegmark. Machine Learning Conservation Laws from Trajectories. *Physical Review Letters*, 126:180604, May 2021.

[32] Christian Loftis, Kunpeng Yuan, Yong Zhao, Ming Hu, and Jianjun Hu. Lattice Thermal Conductivity Prediction Using Symbolic Regression and Machine Learning. *The Journal of Physical Chemistry A*, 125(1):435–450, 2020.

[33] Yoshitomo Matsubara. torchdistill: A Modular, Configuration-Driven Framework for Knowledge Distillation. In *International Workshop on Reproducible Research in Pattern Recognition*, pp. 24–44. Springer, 2021.

[34] Aaron Meurer, Christopher P Smith, Mateusz Paprocki, Ondřej Čertík, Sergey B Kirpichev, Matthew Rocklin, AMiT Kumar, Sergiu Ivanov, Jason K Moore, Sartaj Singh, et al. SymPy: symbolic computing in Python. *PeerJ Computer Science*, 3:e103, 2017.

[35] Shohei Nakai, Tetsuhiro Miyahara, Tetsuji Kuboyama, Tomoyuki Uchida, and Yusuke Suzuki. Acquisition of Characteristic Tree Patterns with VLDC's by Genetic Programming and Edit Distance. In *2013 Second IIAI International Conference on Advanced Applied Informatics*, pp. 147–151. IEEE, 2013.

[36] National Astronomical Observatory of Japan. *Handbook of Scientific Tables*. World Scientific, 2022.

[37] U-M O'Reilly. Using a distance metric on genetic programs to understand genetic operators. In *1997 IEEE International Conference on Systems, Man, and Cybernetics. Computational Cybernetics and Simulation*, volume 5, pp. 4092–4097. IEEE, 1997.

[38] Patryk Orzechowski, William La Cava, and Jason H Moore. Where are we now? A large benchmark study of recent symbolic regression methods. In *Proceedings of the Genetic and Evolutionary Computation Conference*, pp. 1183–1190, 2018.

[39] Adam Paszke, Sam Gross, Francisco Massa, Adam Lerer, James Bradbury, Gregory Chanan, Trevor Killeen, Zeming Lin, Natalia Gimelshein, Luca Antiga, et al. PyTorch: An Imperative Style, High-Performance Deep Learning Library. *Advances in neural information processing systems*, 32:8026–8037, 2019.

[40] Brenden K Petersen, Mikel Landajuela Larma, Terrell N Mundhenk, Claudio Prata Santiago, Soo Kyung Kim, and Joanne Taery Kim. Deep symbolic regression: Recovering mathematical expressions from data via risk-seeking policy gradients. In *International Conference on Learning Representations*, 2020.

[41] Mark Przybocki, Gregory Sanders, and Audrey Le. Edit Distance: A Metric for Machine Translation Evaluation. In *Proceedings of the Fifth International Conference on Language Resources and Evaluation (LREC'06)*, 2006.

[42] Michael Schmidt and Hod Lipson. Distilling Free-Form Natural Laws from Experimental Data. *Science*, 324(5923):81–85, 2009.

[43] Michael Schmidt and Hod Lipson. Age-Fitness Pareto Optimization. In *Genetic programming theory and practice VIII*, pp. 129–146. Springer, 2011.

[44] Matthew D Schwartz. *Quantum Field Theory and the Standard Model*. Cambridge University Press, 2014.

[45] Steven H Strogatz. *Nonlinear Dynamics and Chaos with Student Solutions Manual: With Applications to Physics, Biology, Chemistry, and Engineering*. CRC press, 2018.

[46] Sheng Sun, Runhai Ouyang, Bochao Zhang, and Tong-Yi Zhang. Data-driven discovery of formulas by symbolic regression. *MRS Bulletin*, 44(7):559–564, 2019.

[47] Ilya Sutskever, Oriol Vinyals, and Quoc V Le. Sequence to Sequence Learning with Neural Networks. *Advances in neural information processing systems*, 27, 2014.

[48] Silviu-Marian Udrescu and Max Tegmark. AI Feynman: A physics-inspired method for symbolic regression. *Science Advances*, 6(16):eaay2631, 2020.

[49] Silviu-Marian Udrescu, Andrew Tan, Jiahai Feng, Orisvaldo Neto, Tailin Wu, and Max Tegmark. AI Feynman 2.0: Pareto-optimal symbolic regression exploiting graph modularity. *Advances in Neural Information Processing Systems*, 33, 2020.

[50] Nguyen Quang Uy, Nguyen Xuan Hoai, Michael O'Neill, Robert I McKay, and Edgar Galván-López. Semantically-based Crossover in Genetic Programming: Application to Real-valued Symbolic Regression. *Genetic Programming and Evolvable Machines*, 12(2):91–119, 2011.

[51] Mojtaba Valipour, Bowen You, Maysum Panju, and Ali Ghodsi. SymbolicGPT: A Generative Transformer Model for Symbolic Regression. *arXiv preprint arXiv:2106.14131*, 2021.

[52] Ashish Vaswani, Noam Shazeer, Niki Parmar, Jakob Uszkoreit, Llion Jones, Aidan N Gomez, Łukasz Kaiser, and Illia Polosukhin. Attention Is All You Need. *Advances in neural information processing systems*, 30, 2017.

[53] Marco Virgolin, Tanja Alderliesten, and Peter AN Bosman. Linear scaling with and within semantic backpropagation-based genetic programming for symbolic regression. In *Proceedings of the genetic and evolutionary computation conference*, pp. 1084–1092, 2019.

[54] Marco Virgolin, Tanja Alderliesten, Cees Witteveen, and Peter AN Bosman. Improving Model-Based Genetic Programming for Symbolic Regression of Small Expressions. *Evolutionary computation*, 29(2):211–237, 2021.

[55] Yiqun Wang, Nicholas Wagner, and James M Rondinelli. Symbolic regression in materials science. *MRS Communications*, 9(3):793–805, 2019.

[56] Steven Weinberg. *Gravitation and Cosmology: Principles and Applications of the General Theory of Relativity*. Wiley,, 1972.

[57] Baicheng Weng, Zhilong Song, Rilong Zhu, Qingyu Yan, Qingde Sun, Corey G Grice, Yanfa Yan, and Wan-Jian Yin. Simple descriptor derived from symbolic regression accelerating the discovery of new perovskite catalysts. *Nature Communications*, 11(1):1–8, 2020.

[58] Ronald J Williams and David Zipser. A Learning Algorithm for Continually Running Fully Recurrent Neural Networks. *Neural computation*, 1(2):270–280, 1989.

[59] Tailin Wu and Max Tegmark. Toward an artificial intelligence physicist for unsupervised learning. *Physical Review E*, 100(3):033311, 2019.

[60] Manzil Zaheer, Satwik Kottur, Siamak Ravanbakhsh, Barnabas Poczos, Russ R Salakhutdinov, and Alexander J Smola. Deep sets. In *Neural Information Processing Systems*, 2017.

[61] Kaizhong Zhang and Dennis Shasha. Simple Fast Algorithms for the Editing Distance between Trees and Related Problems. *SIAM journal on computing*, 18(6):1245–1262, 1989.

A Our SRSD Datasets: Additional Information

This section provides additional information regarding our SRSD datasets. We created the datasets to discuss the performance of symbolic regression for scientific discovery (SRSD). We refer readers to Section 3 for details of the datasets. Tables S1 – S11 comprehensively summarize the differences between FSRD and our SRSD datasets. Note that the table of Easy set (part 1) is provided as Table 1 in Section 3.1. As described in Section 3.2.2, we categorized each of the 120 SRSD datasets into one of Easy, Medium, and Hard sets. We published the three sets of the SRSD datasets with MIT License at Hugging Face Dataset repositories. The dataset documentations are publicly available as Hugging Face Dataset cards.^{1, 2, 3} These repositories are version-controlled with Git¹¹ so that users can track the log of the changes.

¹¹<https://git-scm.com/>

Table S1: Easy set of our proposed datasets (part 2). C: Constant, V: Variable, F: Float, I: Integer, P: Positive, N: Negative, NN: Non-Negative, I \star : Integer treated as float due to the capacity of 32-bit integer, \mathcal{U} : Uniform distribution, \mathcal{U}_{\log} : Log-Uniform distribution.

Eq. ID	Formula	Symbols	Properties		Distributions		
			Original	Ours	Original	Ours	
I.30.5	$d = \frac{\lambda}{n \sin \theta}$	d	Interplanar distance	V, F	V, F, P	$\mathcal{U}(2, 5)$	N/A
		λ	Wavelength of X-ray	V, F	V, F, P	$\mathcal{U}(1, 2)$	$\mathcal{U}_{\log}(10^{-11}, 10^{-9})$
		n	The number of phase difference	V, F	V, I, P	$\mathcal{U}(1, 5)$	$\mathcal{U}_{\log}(10^0, 10^2)$
		θ	Incidence/Reflection angle	V, F	V, F	N/A	$\mathcal{U}(-2\pi, 2\pi)$
I.43.16	$v = \mu q \frac{V}{d}$	v	Velocity	V, F	V, F	N/A	N/A
		μ	Ionic conductivity	V, F	V, F	$\mathcal{U}(1, 5)$	$\mathcal{U}_{\log}(10^{-6}, 10^{-4})$
		q	Electric charge of ions	V, F	V, F	$\mathcal{U}(1, 5)$	$\mathcal{U}_{\log}(10^{-11}, 10^{-9})$
		V	Voltage	V, F	V, F	$\mathcal{U}(1, 5)$	$\mathcal{U}_{\log}(10^{-1}, 10^1)$
I.47.23	$c = \sqrt{\frac{\gamma P}{\rho}}$	d	Distance	V, F	V, F, P	$\mathcal{U}(1, 5)$	$\mathcal{U}_{\log}(10^{-3}, 10^{-1})$
		c	Velocity of sound	V, F	V, F, P	N/A	N/A
		γ	Heat capacity ratio	V, F	V, F, P	$\mathcal{U}(1, 5)$	$\mathcal{U}(1, 2)$
		P	Atmospheric pressure	V, F	V, F, P	$\mathcal{U}(1, 5)$	$\mathcal{U}(0.5 \times 10^{-5}, 1.5 \times 10^{-5})$
II.2.42	$J = \kappa(T_2 - T_1) \frac{A}{d}$	ρ	Density of air	V, F	V, F, P	$\mathcal{U}(1, 5)$	$\mathcal{U}(1, 2)$
		J	Energy difference	V, F	V, F	N/A	N/A
		κ	Thermal conductivity	V, F	V, F, P	$\mathcal{U}(1, 5)$	$\mathcal{U}_{\log}(10^{-1}, 10^1)$
		T_2	Temperature	V, F	V, F, P	$\mathcal{U}(1, 5)$	$\mathcal{U}_{\log}(10^1, 10^3)$
II.3.24	$h = \frac{W}{4\pi r^2}$	T_1	Temperature	V, F	V, F, P	$\mathcal{U}(1, 5)$	$\mathcal{U}_{\log}(10^1, 10^3)$
		A	Area	V, F	V, F, P	$\mathcal{U}(1, 5)$	$\mathcal{U}_{\log}(10^{-4}, 10^{-2})$
		d	Length	V, F	V, F, P	$\mathcal{U}(1, 5)$	$\mathcal{U}_{\log}(10^{-2}, 10^0)$
		h	Heat flux	V, F	V, F	N/A	N/A
II.4.23	$\phi = \frac{q}{4\pi\epsilon r}$	W	Work	V, F	V, F	$\mathcal{U}(1, 5)$	$\mathcal{U}_{\log}(10^0, 10^2)$
		r	Distance	V, F	V, F, P	$\mathcal{U}(1, 5)$	$\mathcal{U}_{\log}(10^{-2}, 10^0)$
		ϕ	Electric potential	V, F	V, F	N/A	N/A
		q	Electric charge	V, F	V, F	$\mathcal{U}(1, 5)$	$\mathcal{U}_{\log}(10^{-3}, 10^{-1})$
II.8.31	$u = \frac{\epsilon E^2}{2}$	ϵ	Vacuum permittivity	V, F	C, F, P	$\mathcal{U}(1, 5)$	8.854×10^{-12}
		E	Magnitude of electric field	V, F	V, F, P	$\mathcal{U}(1, 5)$	$\mathcal{U}_{\log}(10^1, 10^3)$
		E	Electric field	V, F	V, F	N/A	N/A
		σ_{free}	Surface charge	V, F	V, F	$\mathcal{U}(1, 5)$	$\mathcal{U}_{\log}(10^{-3}, 10^{-1})$
II.10.9	$E = \frac{\sigma_{\text{free}}}{\epsilon} \frac{1}{1+x}$	ϵ	Vacuum permittivity	V, F	C, F, P	$\mathcal{U}(1, 5)$	8.854×10^{-12}
		x	Electric susceptibility	V, F	V, F, P	$\mathcal{U}(1, 5)$	$\mathcal{U}_{\log}(10^0, 10^2)$
		B	The magnitude of the magnetic field	V, F	V, F	N/A	N/A
		ϵ	Vacuum permittivity	V, F	C, F, P	$\mathcal{U}(1, 5)$	8.854×10^{-12}
II.13.17	$B = \frac{1}{4\pi\epsilon c^2} \frac{2I}{r}$	c	Speed of light	V, F	C, F, P	$\mathcal{U}(1, 5)$	2.998×10^8
		I	Electric current	V, F	V, F	$\mathcal{U}(1, 5)$	$\mathcal{U}_{\log}(10^{-3}, 10^{-1})$
		r	Radius	V, F	V, F, P	$\mathcal{U}(1, 5)$	$\mathcal{U}_{\log}(10^{-3}, 10^{-1})$
		U	Energy from magnetic field	V, F	V, F	N/A	N/A
II.15.4	$U = -\mu B \cos \theta$	μ	Magnetic dipole moment	V, F	V, F	$\mathcal{U}(1, 5)$	$\mathcal{U}_{\log}(10^{-25}, 10^{-23})$
		B	Magnetic field strength	V, F	V, F	$\mathcal{U}(1, 5)$	$\mathcal{U}_{\log}(10^{-3}, 10^{-1})$
		θ	Angle	V, F	V, F, NN	$\mathcal{U}(1, 5)$	$\mathcal{U}(0, 2\pi)$

Table S2: Easy set of our proposed datasets (part 3).

Eq. ID	Formula	Symbols	Properties		Distributions	
			Original	Ours	Original	Ours
II.15.5	$U = -pE \cos \theta$	U Energy	V, F	V, F	N/A	N/A
		p Electric dipole moment	V, F	V, F	$\mathcal{U}(1, 5)$	$\mathcal{U}_{\log}(10^{-22}, 10^{-20})$
		E Magnitude of electric field	V, F	V, F	$\mathcal{U}(1, 5)$	$\mathcal{U}_{\log}(10^1, 10^3)$
		θ Angle	V, F	V, F	$\mathcal{U}(1, 5)$	$\mathcal{U}(0, 2\pi)$
II.27.16	$S = \epsilon c E^2$	S Radiant intensity	V, F	V, F	N/A	N/A
		ϵ Vacuum permittivity	V, F	C, F, P	$\mathcal{U}(1, 5)$	8.854×10^{-12}
		c Speed of light	V, F	C, F, P	$\mathcal{U}(1, 5)$	2.998×10^8
		E Magnitude of electric field	V, F	V, F, P	$\mathcal{U}(1, 5)$	$\mathcal{U}_{\log}(10^{-1}, 10^1)$
II.27.18	$u = \epsilon E^2$	u Energy density	V, F	V, F, P	N/A	N/A
		ϵ Vacuum permittivity	V, F	C, F, P	$\mathcal{U}(1, 5)$	8.854×10^{-12}
		E Magnitude of electric field	V, F	V, F, P	$\mathcal{U}(1, 5)$	$\mathcal{U}_{\log}(10^{-1}, 10^1)$
II.34.11	$\omega = g \frac{qB}{2m}$	ω Angular frequency	V, F	V, F	N/A	N/A
		g g-factor	V, F	V, F	$\mathcal{U}(1, 5)$	$\mathcal{U}(-1, 1)$
		q Electric charge	V, F	V, F	$\mathcal{U}(1, 5)$	$\mathcal{U}_{\log}(10^{-11}, 10^{-9})$
		B Magnetic field strength	V, F	V, F	$\mathcal{U}(1, 5)$	$\mathcal{U}_{\log}(10^{-9}, 10^{-7})$
		m Mass	V, F	V, F, P	$\mathcal{U}(1, 5)$	$\mathcal{U}_{\log}(10^{-30}, 10^{-28})$
II.34.29b	$U = 2\pi g\mu B \frac{J_z}{\hbar}$	U Energy	V, F	V, F, P	N/A	N/A
		g g-factor	V, F	V, F	$\mathcal{U}(1, 5)$	$\mathcal{U}(-1, 1)$
		μ Bohr magneton	V, F	C, F, P	$\mathcal{U}(1, 5)$	$9.2740100783 \times 10^{-24}$
		B Magnetic field strength	V, F	V, F	$\mathcal{U}(1, 5)$	$\mathcal{U}_{\log}(10^{-3}, 10^{-1})$
		J_z Element of angular momentum	V, F	V, F	$\mathcal{U}(1, 5)$	$\mathcal{U}_{\log}(10^{-26}, 10^{-22})$
II.38.3	$F = YA \frac{\Delta l}{l}$	h Planck constant	V, F	C, F, P	$\mathcal{U}(1, 5)$	6.626×10^{-34}
		F Force	V, F	V, F	N/A	N/A
		Y Young's modulus	V, F	V, F, P	$\mathcal{U}(1, 5)$	$\mathcal{U}_{\log}(10^{-1}, 10^1)$
		A Area	V, F	V, F, P	$\mathcal{U}(1, 5)$	$\mathcal{U}_{\log}(10^{-4}, 10^{-2})$
		δl Displacement	V, F	V, F	$\mathcal{U}(1, 5)$	$\mathcal{U}_{\log}(10^{-3}, 10^{-1})$
II.38.14	$\mu = \frac{Y}{2(1+\sigma)}$	l Length	V, F	V, F, P	$\mathcal{U}(1, 5)$	$\mathcal{U}_{\log}(10^{-2}, 10^0)$
		μ Rigidity modulus	V, F	V, F, P	N/A	N/A
		Y Young's modulus	V, F	V, F, P	$\mathcal{U}(1, 5)$	$\mathcal{U}_{\log}(10^{-1}, 10^1)$
		σ Poisson coefficient	V, F	V, F, P	$\mathcal{U}(1, 5)$	$\mathcal{U}_{\log}(10^{-2}, 10^0)$
III.7.38	$\omega = \frac{4\pi\mu B}{h}$	ω Precession frequency	V, F	V, F	N/A	N/A
		μ Magnetic moment	V, F	V, F	$\mathcal{U}(1, 5)$	$\mathcal{U}_{\log}(10^{-11}, 10^{-9})$
		B Magnetic flux density	V, F	V, F	$\mathcal{U}(1, 5)$	$\mathcal{U}_{\log}(10^{-3}, 10^{-1})$
		h Planck constant	V, F	C, F, P	$\mathcal{U}(1, 5)$	6.626×10^{-34}
III.12.43	$J = \frac{mh}{2\pi}$	J Variable	V, F	V, F	N/A	N/A
		m Spin state	V, F	V, I, NNN	$\mathcal{U}(1, 5)$	$\mathcal{U}_{\log}(10^0, 10^2)$
		h Planck constant	V, F	C, F, P	$\mathcal{U}(1, 5)$	6.626×10^{-34}
III.15.27	$k = \frac{2\pi}{Nb} s$	k Wavenumber	V, F	V, F	N/A	N/A
		s Parameter of state	V, F	V, I	$\mathcal{U}(1, 5)$	$\mathcal{U}_{\log}(10^0, 10^2)$
		N Number of atoms	V, F	V, I, P	$\mathcal{U}(1, 5)$	$\mathcal{U}_{\log}(10^0, 10^2)$
		b Lattice constant	V, F	V, F, P	$\mathcal{U}(1, 5)$	$\mathcal{U}_{\log}(10^{-10}, 10^{-8})$

Table S3: Medium set of our proposed datasets (part 1).

Eq. ID	Formula	Symbols	Properties		Distributions	
			Original	Ours	Original	Ours
I.8.14	$d = \sqrt{(x_2 - x_1)^2 + (y_2 - y_1)^2}$	d	Distance	V, F	V, F, NN	N/A
		x_2	Position	V, F	V, F	$\mathcal{U}(1, 5)$
		x_1	Position	V, F	V, F	$\mathcal{U}(1, 5)$
		y_2	Position	V, F	V, F	$\mathcal{U}(1, 5)$
		y_1	Position	V, F	V, F	$\mathcal{U}(1, 5)$
I.10.7	$m = \frac{m_0}{\sqrt{1 - \frac{v^2}{c^2}}}$	m	Mass	V, F	V, F, P	N/A
		m_0	Invariant mass	V, F	V, F, P	$\mathcal{U}(1, 5)$
		v	Velocity	V, F	V, F, P	$\mathcal{U}(1, 2)$
		c	Speed of light	V, F	C, F, P	$\mathcal{U}(3, 10)$
I.11.19	$A = x_1 y_1 + x_2 y_2 + x_3 y_3$	A	Inner product	V, F	V, F	N/A
		x_1	Element of a vector	V, F	V, F	$\mathcal{U}(1, 5)$
		y_1	Element of a vector	V, F	V, F	$\mathcal{U}(1, 5)$
		x_2	Element of a vector	V, F	V, F	$\mathcal{U}(1, 5)$
		y_2	Element of a vector	V, F	V, F	$\mathcal{U}(1, 5)$
		x_3	Element of a vector	V, F	V, F	$\mathcal{U}(1, 5)$
		y_3	Element of a vector	V, F	V, F	$\mathcal{U}(1, 5)$
		F	Electrostatic force	V, F	V, F	N/A
I.12.2	$F = \frac{q_1 q_2}{4\pi\epsilon r^2}$	q_1	Electric charge	V, F	V, F	$\mathcal{U}(1, 5)$
		q_2	Electric charge	V, F	V, F	$\mathcal{U}(1, 5)$
		r	Distance	V, F	V, F, P	$\mathcal{U}(1, 5)$
		ϵ	Vacuum permittivity	V, F	C, F, P	8.854×10^{-12}
I.12.11	$F = q(E + Bv \sin(\theta))$	F	Force	V, F	V, F	N/A
		q	Electric charge	V, F	V, F	$\mathcal{U}(1, 5)$
		E	Electric field	V, F	V, F	$\mathcal{U}(1, 5)$
		B	Magnetic field strength	V, F	V, F, P	$\mathcal{U}(1, 5)$
		v	Velocity	V, F	V, F, P	$\mathcal{U}(1, 5)$
		θ	Angle	V, F	V, F, NN	$\mathcal{U}(1, 5)$
I.13.4	$K = \frac{1}{2}m(v^2 + u^2 + w^2)$	K	Kinetic energy	V, F	V, F, P	N/A
		m	Mass	V, F	V, F, P	$\mathcal{U}(1, 5)$
		v	Element of velocity	V, F	V, F, P	$\mathcal{U}(1, 5)$
		u	Element of velocity	V, F	V, F, P	$\mathcal{U}(1, 5)$
		w	Element of velocity	V, F	V, F, P	$\mathcal{U}(1, 5)$
I.13.12	$U = Gm_1 m_2 \left(\frac{1}{r_2} - \frac{1}{r_1} \right)$	U	Potential energy	V, F	V, F, P	N/A
		G	Gravitational constant	V, F	C, F, P	$\mathcal{U}(1, 5)$
		m_1	Mass (The Earth)	V, F	V, F, P	$\mathcal{U}(1, 5)$
		m_2	Mass	V, F	V, F, P	$\mathcal{U}(1, 5)$
		r_2	Distance	V, F	V, F, P	$\mathcal{U}(1, 5)$
		r_1	Distance	V, F	V, F, P	$\mathcal{U}(1, 5)$
I.15.10	$p = \frac{m_0 v}{\sqrt{1 - v^2/c^2}}$	p	Relativistic mass	V, F	V, F, P	N/A
		m_0	Rest Mass	V, F	V, F, P	$\mathcal{U}(1, 5)$
		v	Velocity	V, F	V, F	$\mathcal{U}(1, 2)$
		c	Speed of light	V, F	C, F, P	$\mathcal{U}(3, 10)$
I.16.6	$v_1 = \frac{u+v}{1+uv/c^2}$	v_1	Velocity	V, F	V, F	N/A
		u	Velocity	V, F	V, F	$\mathcal{U}(1, 5)$
		v	Velocity	V, F	V, F	$\mathcal{U}(1, 5)$
		c	Speed of light	V, F	C, F, P	$\mathcal{U}(1, 5)$
I.18.4	$r = \frac{m_1 r_1 + m_2 r_2}{m_1 + m_2}$	r	Center of gravity	V, F	V, F	N/A
		m_1	Mass	V, F	V, F, P	$\mathcal{U}(1, 5)$
		r_1	Position	V, F	V, F	$\mathcal{U}(1, 5)$
		m_2	Mass	V, F	V, F, P	$\mathcal{U}(1, 5)$
		r_2	Position	V, F	V, F	$\mathcal{U}(1, 5)$

Table S4: Medium set of our proposed datasets (part 2).

Eq. ID	Formula	Symbols	Properties		Distributions	
			Original	Ours	Original	Ours
I.24.6	$E = \frac{1}{4}m(\omega^2 + \omega_0^2)x^2$	E Energy	V, F	V, F, P	N/A	N/A
		m Mass	V, F	V, F, P	$\mathcal{U}(1, 3)$	$\mathcal{U}_{\log}(10^{-1}, 10^1)$
		ω Angular velocity	V, F	V, F	$\mathcal{U}(1, 3)$	$\mathcal{U}_{\log}(10^{-1}, 10^1)$
		ω_0 Angular velocity	V, F	V, F	$\mathcal{U}(1, 3)$	$\mathcal{U}_{\log}(10^{-1}, 10^1)$
I.29.4	$k = \frac{\omega}{c}$	x Position	V, F	V, F	$\mathcal{U}(1, 3)$	$\mathcal{U}_{\log}(10^{-1}, 10^1)$
		k Wavenumber	V, F	V, F, P	N/A	N/A
		ω Frequency of electromagnetic waves	V, F	V, F, P	$\mathcal{U}(1, 10)$	$\mathcal{U}_{\log}(10^9, 10^{11})$
I.32.5	$P = \frac{q^2 a^2}{6\pi\epsilon c^3}$	c Speed of light	V, F	C, F, P	$\mathcal{U}(1, 10)$	2.998×10^8
		P Radian energy	V, F	V, F, P	N/A	N/A
		q Electric charge	V, F	V, F	$\mathcal{U}(1, 5)$	$\mathcal{U}_{\log}(10^{-3}, 10^{-1})$
		a Magnitude of direction vector	V, F	V, F, P	$\mathcal{U}(1, 5)$	$\mathcal{U}_{\log}(10^5, 10^7)$
I.34.8	$\omega = \frac{qvB}{p}$	ϵ Vacuum permittivity	V, F	C, F, P	$\mathcal{U}(1, 5)$	8.854×10^{-12}
		c Speed of light	V, F	C, F, P	$\mathcal{U}(1, 5)$	2.998×10^8
		ω Angular velocity	V, F	V, F	N/A	N/A
		q Electric charge	V, F	V, F	$\mathcal{U}(1, 5)$	$\mathcal{U}_{\log}(10^{-11}, 10^{-9})$
I.34.10	$\omega = \frac{\omega_0}{1-v/c}$	v Velocity	V, F	V, F	$\mathcal{U}(1, 5)$	$\mathcal{U}_{\log}(10^5, 10^7)$
		B Magnetic field	V, F	V, F	$\mathcal{U}(1, 5)$	$\mathcal{U}_{\log}(10^1, 10^3)$
		p Angular momentum	V, F	V, F	$\mathcal{U}(1, 5)$	$\mathcal{U}_{\log}(10^9, 10^{11})$
		ω Frequency of electromagnetic waves	V, F	V, F, P	N/A	N/A
I.34.27	$W = \frac{h}{2\pi}\omega$	ω_0 Frequency of electromagnetic waves	V, F	V, F, P	$\mathcal{U}(1, 5)$	$\mathcal{U}_{\log}(10^9, 10^{11})$
		v Velocity	V, F	V, F	$\mathcal{U}(1, 2)$	$\mathcal{U}_{\log}(10^5, 10^7)$
		c Speed of light	V, F	C, F, P	$\mathcal{U}(3, 10)$	2.998×10^8
I.38.12	$r = 4\pi\epsilon \frac{(h/(2\pi))^2}{mq^2}$	W Energy	V, F	V, F, P	N/A	N/A
		h Planck constant	V, F	C, F, P	$\mathcal{U}(1, 5)$	6.626×10^{-34}
		ω Frequency of electromagnetic waves	V, F	V, F, P	$\mathcal{U}(1, 5)$	$\mathcal{U}_{\log}(10^9, 10^{11})$
		r Bohr radius	V, F	V, F, P	N/A	N/A
I.39.10	$U = \frac{3}{2}PV$	ϵ Vacuum permittivity	V, F	C, F, P	$\mathcal{U}(1, 5)$	8.854×10^{-12}
		h Planck constant	V, F	C, F, P	$\mathcal{U}(1, 5)$	6.626×10^{-34}
		m Mass	V, F	V, F, P	$\mathcal{U}(1, 5)$	$\mathcal{U}_{\log}(10^{-28}, 10^{-26})$
		q Electric charge	V, F	V, F	$\mathcal{U}(1, 5)$	$\mathcal{U}_{\log}(10^{-11}, 10^{-9})$
I.39.11	$U = \frac{PV}{\gamma-1}$	U Internal energy	V, F	V, F, P	N/A	N/A
		P Pressure	V, F	V, F, P	$\mathcal{U}(1, 5)$	$\mathcal{U}_{\log}(10^4, 10^6)$
		V Volume	V, F	V, F, P	$\mathcal{U}(1, 5)$	$\mathcal{U}_{\log}(10^{-5}, 10^{-3})$
I.39.11	$U = \frac{PV}{\gamma-1}$	U Energy	V, F	V, F	N/A	N/A
		γ Heat capacity ratio	V, F	V, F, P	$\mathcal{U}(2, 5)$	$\mathcal{U}(1, 2)$
		P Pressure	V, F	V, F, P	$\mathcal{U}(1, 5)$	$\mathcal{U}_{\log}(10^4, 10^6)$
		V Volume	V, F	V, F, P	$\mathcal{U}(1, 5)$	$\mathcal{U}_{\log}(10^{-5}, 10^{-3})$
I.43.31	$D = \mu kT$	D Diffusion coefficient	V, F	V, F, P	N/A	N/A
		μ Viscosity	V, F	V, F, P	$\mathcal{U}(1, 5)$	$\mathcal{U}_{\log}(10^{13}, 10^{15})$
		k Boltzmann constant	V, F	C, F, P	$\mathcal{U}(1, 5)$	1.381×10^{-23}
		T Temperature	V, F	V, F, P	$\mathcal{U}(1, 5)$	$\mathcal{U}_{\log}(10^1, 10^3)$

Table S5: Medium set of our proposed datasets (part 3).

Eq. ID	Formula	Symbols	Properties		Distributions	
			Original	Ours	Original	Ours
I.43.43	$\kappa = \frac{1}{\gamma-1} \frac{kv}{\sigma_c}$	κ	Thermal conductivity	V, F	V, F, P	N/A
		γ	Heat capacity ratio	V, F	V, F, P	$\mathcal{U}(2, 5)$
		k	Boltzmann constant	V, F	C, F, P	$\mathcal{U}(1, 5)$
		v	Velocity	V, F	V, F, P	$\mathcal{U}(1, 5)$
I.48.2	$E = \frac{mc^2}{\sqrt{1-v^2/c^2}}$	σ_c	Molecular collision cross section	V, F	V, F, P	$\mathcal{U}(1, 5)$
		E	Energy	V, F	V, F, P	N/A
		m	Mass	V, F	V, F, P	$\mathcal{U}(1, 5)$
		c	Speed of light	V, F	C, F, P	$\mathcal{U}(3, 10)$
II.6.11	$\phi = \frac{1}{4\pi\epsilon} \frac{p \cos \theta}{r^2}$	v	Velocity	V, F	V, F, P	$\mathcal{U}(1, 2)$
		ϕ	Electric potential	V, F	V, F	N/A
		ϵ	Vacuum permittivity	V, F	C, F, P	$\mathcal{U}(1, 3)$
		p	Electric dipole moment	V, F	V, F	$\mathcal{U}(1, 3)$
II.8.7	$U = \frac{3}{5} \frac{Q^2}{4\pi\epsilon a}$	θ	Angle	V, F	V, F, NN	$\mathcal{U}(1, 3)$
		r	Distance	V, F	V, F, P	$\mathcal{U}(1, 3)$
		U	Energy	V, F	V, F	N/A
		Q	Electric charge	V, F	V, F	$\mathcal{U}(1, 5)$
II.11.3	$x = \frac{qE}{m(\omega_0^2 - \omega^2)}$	ϵ	Vacuum permittivity	V, F	C, F, P	$\mathcal{U}(1, 5)$
		a	Radius	V, F	V, F, P	$\mathcal{U}(1, 5)$
		x	Position	V, F	V, F	N/A
		q	Electric charge	V, F	V, F	$\mathcal{U}(1, 3)$
II.21.32	$\phi = \frac{q}{4\pi\epsilon r(1-v/c)}$	E	Magnitude of electric field	V, F	V, F, P	$\mathcal{U}(1, 3)$
		m	Mass	V, F	V, F, P	$\mathcal{U}(1, 3)$
		ω_0	Angular velocity	V, F	V, F	$\mathcal{U}(3, 5)$
		ω	Angular velocity	V, F	V, F	$\mathcal{U}(1, 2)$
II.34.2	$\mu = \frac{qv r}{2}$	ϕ	Electric potential	V, F	V, F	N/A
		q	Electric charge	V, F	V, F	$\mathcal{U}(1, 5)$
		ϵ	Vacuum permittivity	V, F	C, F, P	$\mathcal{U}(1, 5)$
		r	Distance	V, F	V, F, P	$\mathcal{U}(1, 5)$
II.34.2a	$I = \frac{qv}{2\pi r}$	v	Velocity	V, F	V, F, P	$\mathcal{U}(1, 2)$
		c	Speed of light	V, F	C, F, P	$\mathcal{U}(3, 10)$
		μ	Magnetic moment	V, F	V, F	N/A
		q	Electric charge	V, F	V, F	$\mathcal{U}(1, 5)$
II.34.29a	$\mu = \frac{gh}{4\pi m}$	v	Velocity	V, F	V, F	$\mathcal{U}(1, 5)$
		r	Radius	V, F	V, F, P	$\mathcal{U}(1, 5)$
		I	Electric Current	V, F	V, F	N/A
		q	Electric charge	V, F	V, F	$\mathcal{U}(1, 5)$
II.37.1	$E = \mu(1 + \chi)B$	v	Velocity	V, F	V, F	$\mathcal{U}(1, 5)$
		r	Radius	V, F	V, F, P	$\mathcal{U}(1, 5)$
		μ	Magnetic moment	V, F	V, F	$\mathcal{U}(1, 5)$
		χ	Volume magnetic susceptibility	V, F	V, F	$\mathcal{U}(1, 5)$
		B	Magnetic field strength	V, F	V, F	$\mathcal{U}(1, 5)$
		E	Energy of magnetic field	V, F	V, F	N/A
		μ	Magnetic moment	V, F	V, F	$\mathcal{U}(1, 5)$
		χ	Volume magnetic susceptibility	V, F	V, F	$\mathcal{U}(1, 5)$
		B	Magnetic field strength	V, F	V, F	$\mathcal{U}(1, 5)$

Table S6: Medium set of our proposed datasets (part 4).

Eq. ID	Formula	Symbols	Properties		Distributions	
			Original	Ours	Original	Ours
III.4.32	$n = \frac{1}{\exp(\hbar\omega/2\pi kT)-1}$	n	Average number of photons	V, F	V, F, P	N/A
		\hbar	Planck constant	V, F	C, F, P	$\mathcal{U}(1, 5)$
		ω	Frequency	V, F	V, F, P	$\mathcal{U}(1, 5)$
		k	Boltzmann constant	V, F	C, F, P	$\mathcal{U}(1, 5)$
III.8.54	$ C ^2 = \sin^2\left(\frac{2\pi At}{\hbar}\right)$	T	Temperature	V, F	V, F, P	$\mathcal{U}(1, 5)$
		$ C ^2$	Probability	V, F	V, F, NN	N/A
		A	Energy	V, F	V, F	$\mathcal{U}(1, 2)$
		t	Time	V, F	V, F, NN	$\mathcal{U}(1, 2)$
III.13.18	$v = \frac{4\pi Ab^2}{h} k$	h	Planck constant	V, F	C, F, P	$\mathcal{U}(1, 4)$
		v	Speed of the waves	V, F	V, F	N/A
		A	Energy	V, F	V, F	$\mathcal{U}(1, 5)$
		b	Lattice constant	V, F	V, F, P	$\mathcal{U}(1, 5)$
III.14.14	$I = I_0 (\exp(q\Delta V/\kappa T) - 1)$	k	Wavenumber	V, F	V, F, P	$\mathcal{U}(1, 5)$
		h	Planck constant	V, F	C, F, P	$\mathcal{U}(1, 5)$
		I	Electric Current	V, F	V, F	N/A
		I_0	Electric current	V, F	V, F	$\mathcal{U}(1, 5)$
III.14.14	$I = I_0 (\exp(q\Delta V/\kappa T) - 1)$	q	Electric charge	V, F	V, F, P	$\mathcal{U}(1, 2)$
		ΔV	Voltage	V, F	V, F	$\mathcal{U}(1, 2)$
		κ	Boltzmann constant	V, F	C, F, P	$\mathcal{U}(1, 2)$
		T	Temperature	V, F	V, F, P	$\mathcal{U}(1, 2)$
III.15.12	$E = 2A(1 - \cos(kd))$	E	Energy	V, F	V, F, P	N/A
		A	Amplitude	V, F	V, F, P	$\mathcal{U}(1, 5)$
		k	Propagation coefficient	V, F	V, F, P	$\mathcal{U}(1, 5)$
		d	Lattice constant	V, F	V, F, P	$\mathcal{U}(1, 5)$
III.15.14	$m = \frac{h^2}{8\pi^2 Ab^2}$	m	Effective mass	V, F	V, F, P	N/A
		h	Planck constant	V, F	C, F, P	$\mathcal{U}(1, 5)$
		A	Amplitude	V, F	V, F, P	$\mathcal{U}(1, 5)$
		b	Lattice constant	V, F	V, F, P	$\mathcal{U}(1, 5)$
III.17.37	$f = \beta(1 + \alpha \cos \theta)$	f	Distribution	V, F	V, F	N/A
		β	Variable	V, F	V, F, P	$\mathcal{U}(1, 5)$
		α	Variable	V, F	V, F	$\mathcal{U}(1, 5)$
		θ	Angle	V, F	V, F, NN	$\mathcal{U}(1, 5)$
III.19.51	$E = -\frac{mq^4}{2(4\pi\epsilon)^2(h/(2\pi))^2n^2}$	E	Energy	V, F	V, F, P	N/A
		m	Mass	V, F	V, F, P	$\mathcal{U}(1, 5)$
		q	Electric charge	V, F	V, F	$\mathcal{U}(1, 5)$
		ϵ	Vacuum permittivity	V, F	C, F, P	$\mathcal{U}(1, 5)$
B8	$U = \frac{E}{1 + \frac{E}{mc^2}(1 - \cos \theta)}$	h	Planck constant	V, F	C, F, P	$\mathcal{U}(1, 5)$
		n	Number of protons	V, F	V, I, P	$\mathcal{U}(1, 5)$
		U	Variable	V, F	V, F, P	N/A
		E	Electromagnetic energy	V, F	V, F, P	$\mathcal{U}(1, 3)$
B18	$\rho = \frac{3}{8\pi G} \left(\frac{c^2 k_f}{a_f^2} + H^2 \right)$	m	Electron mass	V, F	C, F, P	$\mathcal{U}(1, 3)$
		c	Speed of light	V, F	C, F, P	$\mathcal{U}(1, 3)$
		θ	Incidence angle	V, F	V, F	$\mathcal{U}(1, 3)$
		ρ	Variable	V, F	V, F	N/A
B18	$\rho = \frac{3}{8\pi G} \left(\frac{c^2 k_f}{a_f^2} + H^2 \right)$	G	Gravitational constant	V, F	C, F, P	$\mathcal{U}(1, 5)$
		c	Speed of light	V, F	C, F, P	$\mathcal{U}(1, 5)$
		k_f	Variable	V, F	V, F	$\mathcal{U}(1, 5)$
		a_f	Distance	V, F	V, F, P	$\mathcal{U}(1, 5)$
B18	$\rho = \frac{3}{8\pi G} \left(\frac{c^2 k_f}{a_f^2} + H^2 \right)$	H	Variable	V, F	V, F	$\mathcal{U}(1, 5)$

Table S7: Hard set of our proposed datasets (part 1).

Eq. ID	Formula	Symbols	Properties		Distributions	
			Original	Ours	Original	Ours
I.6.20	$f = \exp\left(-\frac{\theta^2}{2\sigma^2}\right) / \sqrt{2\pi\sigma^2}$	f Probability density function	V, F	V, F	N/A	N/A
		θ Position	V, F	V, F	$\mathcal{U}(1, 3)$	$\mathcal{U}_{\log}(10^{-1}, 10^1)$
		σ Standard deviation	V, F	V, F, P	$\mathcal{U}(1, 3)$	$\mathcal{U}_{\log}(10^{-1}, 10^1)$
I.6.20a	$f = \exp\left(-\frac{\theta^2}{2}\right) / \sqrt{2\pi}$	f Probability density function	V, F	V, F	N/A	N/A
		θ Position	V, F	V, F	$\mathcal{U}(1, 3)$	$\mathcal{U}_{\log}(10^{-1}, 10^1)$
I.6.20b	$f = \exp\left(-\frac{(\theta - \theta_1)^2}{2\sigma^2}\right) / \sqrt{2\pi\sigma}$	f Probability density function	V, F	V, F	N/A	N/A
		θ Position	V, F	V, F	$\mathcal{U}(1, 3)$	$\mathcal{U}_{\log}(10^{-1}, 10^1)$
		θ_1 Position	V, F	V, F	$\mathcal{U}(1, 3)$	$\mathcal{U}_{\log}(10^{-1}, 10^1)$
		σ Standard deviation	V, F	V, F, P	$\mathcal{U}(1, 3)$	$\mathcal{U}_{\log}(10^{-1}, 10^1)$
I.9.18	$F = \frac{Gm_1m_2}{(x_2 - x_1)^2 + (y_2 - y_1)^2 + (z_2 - z_1)^2} x_1$	F Force of gravity	V, F	V, F	N/A	N/A
		G Gravitational constant	V, F	C, F, P	$\mathcal{U}(1, 2)$	6.674×10^{-11}
		m_1 Mass	V, F	V, F, P	$\mathcal{U}(1, 2)$	$\mathcal{U}_{\log}(10^0, 10^3)$
		m_2 Mass	V, F	V, F, P	$\mathcal{U}(1, 2)$	$\mathcal{U}_{\log}(10^0, 10^3)$
		x_2 Position	V, F	V, F	$\mathcal{U}(1, 2)$	$\mathcal{U}_{\log}(10^0, 10^1)$
		x_1 Position	V, F	V, F	$\mathcal{U}(3, 4)$	$\mathcal{U}_{\log}(10^0, 10^1)$
		y_2 Position	V, F	V, F	$\mathcal{U}(1, 2)$	$\mathcal{U}_{\log}(10^0, 10^1)$
		y_1 Position	V, F	V, F	$\mathcal{U}(3, 4)$	$\mathcal{U}_{\log}(10^0, 10^1)$
		z_2 Position	V, F	V, F	$\mathcal{U}(1, 2)$	$\mathcal{U}_{\log}(10^0, 10^1)$
		z_1 Position	V, F	V, F	$\mathcal{U}(3, 4)$	$\mathcal{U}_{\log}(10^0, 10^1)$
I.15.3t	$t_1 = \frac{t - ux/c^2}{\sqrt{1 - u^2/c^2}}$	t_1 Time	V, F	V, F	N/A	N/A
		t Time	V, F	V, F, NN	$\mathcal{U}(1, 5)$	$\mathcal{U}_{\log}(10^{-6}, 10^{-4})$
		u Velocity	V, F	V, F	$\mathcal{U}(1, 2)$	$\mathcal{U}_{\log}(10^5, 10^7)$
		x Position	V, F	V, F	$\mathcal{U}(1, 5)$	$\mathcal{U}_{\log}(10^0, 10^2)$
I.15.3x	$x_1 = \frac{x - ut}{\sqrt{1 - u^2/c^2}}$	c Speed of light	V, F	C, F, P	$\mathcal{U}(3, 10)$	2.998×10^8
		x_1 Position	V, F	V, F	N/A	N/A
		x Position	V, F	V, F	$\mathcal{U}(5, 10)$	$\mathcal{U}_{\log}(10^0, 10^2)$
		u Velocity	V, F	V, F	$\mathcal{U}(1, 2)$	$\mathcal{U}_{\log}(10^6, 10^8)$
		t Time	V, F	V, F	$\mathcal{U}(1, 2)$	$\mathcal{U}_{\log}(10^{-6}, 10^{-4})$
I.29.16	$x = \sqrt{x_1^2 + x_2^2 + 2x_1x_2 \cos(\theta_1 - \theta_2)}$	c Speed of light	V, F	C, F, P	$\mathcal{U}(3, 20)$	2.998×10^8
		x Wavelength	V, F	V, F, P	N/A	N/A
		x_1 Wavelength	V, F	V, F, P	$\mathcal{U}(1, 5)$	$\mathcal{U}_{\log}(10^{-1}, 10^1)$
		x_2 Wavelength	V, F	V, F, P	$\mathcal{U}(1, 5)$	$\mathcal{U}_{\log}(10^{-1}, 10^1)$
		θ_1 Angle	V, F	V, F, NN	$\mathcal{U}(1, 5)$	$\mathcal{U}(0, 2\pi)$
		θ_2 Angle	V, F	V, F, NN	$\mathcal{U}(1, 5)$	$\mathcal{U}(0, 2\pi)$
		I Amplitude of combined wave	V, F	V, F	N/A	N/A
I.30.3	$I = I_0 \frac{\sin^2(n\theta/2)}{\sin^2(\theta/2)}$	I_0 Amplitude of wave	V, F	V, F, P	$\mathcal{U}(1, 5)$	$\mathcal{U}_{\log}(10^{-3}, 10^{-1})$
		n The number of waves	V, F	V, I, P	$\mathcal{U}(1, 5)$	$\mathcal{U}_{\log}(10^1, 10^3)$
		θ Phase difference	V, F	V, F	$\mathcal{U}(1, 5)$	$\mathcal{U}(-2\pi, 2\pi)$
		P Energy	V, F	V, F, P	N/A	N/A
I.32.17	$P = \left(\frac{1}{2}\epsilon c E^2\right) \left(\frac{8\pi r^2}{3}\right) \left(\frac{\omega^4}{(\omega^2 - \omega_0^2)^2}\right)$	ϵ Vacuum permittivity	V, F	C, F, P	$\mathcal{U}(1, 2)$	8.854×10^{-12}
		c Speed of light	V, F	C, F, P	$\mathcal{U}(1, 2)$	2.998×10^8
		E Magnitude of electric field	V, F	V, F, P	$\mathcal{U}(1, 2)$	$\mathcal{U}_{\log}(10^1, 10^3)$
		r Radius	V, F	V, F, P	$\mathcal{U}(1, 2)$	$\mathcal{U}_{\log}(10^{-2}, 10^0)$
		ω Frequency of electromagnetic waves	V, F	V, F	$\mathcal{U}(1, 2)$	$\mathcal{U}_{\log}(10^9, 10^{11})$
		ω_0 Frequency of electromagnetic waves	V, F	V, F	$\mathcal{U}(3, 5)$	$\mathcal{U}_{\log}(10^9, 10^{11})$
		ω Frequency of electromagnetic waves	V, F	V, F	N/A	N/A
		v Velocity	V, F	V, F	$\mathcal{U}(1, 2)$	$\mathcal{U}_{\log}(10^6, 10^8)$
I.34.14	$\omega = \frac{1+v/c}{\sqrt{1-v^2/c^2}} \omega_0$	c Speed of light	V, F	C, F, P	$\mathcal{U}(3, 10)$	2.998×10^8
		ω_0 Frequency of electromagnetic waves	V, F	V, F, P	$\mathcal{U}(1, 5)$	$\mathcal{U}_{\log}(10^9, 10^{11})$

Table S8: Hard set of our proposed datasets (part 2).

Eq. ID	Formula	Symbols	Properties		Distributions	
			Original	Ours	Original	Ours
I.37.4	$I_{12} = I_1 + I_2 + 2\sqrt{I_1 I_2} \cos \delta$	I_{12}	Amplitude of wave	V, F	V, F, P	N/A
		I_1	Amplitude of wave	V, F	V, F, P	$\mathcal{U}(1, 5) \mathcal{U}_{\log}(10^{-1}, 10^{-3})$
		I_2	Amplitude of wave	V, F	V, F, P	$\mathcal{U}(1, 5) \mathcal{U}_{\log}(10^{-1}, 10^{-3})$
		δ	Phase difference	V, F	V, F	$\mathcal{U}(1, 5) \mathcal{U}(0, \pi)$
I.39.22	$P = \frac{n k T}{V}$	P	Pressure	V, F	V, F, P	N/A
		n	Number of molecules	V, F	V, I*, P	$\mathcal{U}(1, 5) \mathcal{U}_{\log}(10^{23}, 10^{25})$
		k	Boltzmann constant	V, F	C, F, P	$\mathcal{U}(1, 5) 1.381 \times 10^{-23}$
		T	Temperature	V, F	V, F, P	$\mathcal{U}(1, 5) \mathcal{U}_{\log}(10^1, 10^3)$
I.40.1	$n = n_0 \exp(-mgx/kT)$	n	Molecular density	V, F	V, F, P	N/A
		n_0	Molecular density	V, F	V, F, P	$\mathcal{U}(1, 5) \mathcal{U}_{\log}(10^{25}, 10^{27})$
		m	Mass	V, F	V, F, P	$\mathcal{U}(1, 5) \mathcal{U}_{\log}(10^{-24}, 10^{-22})$
		g	Gravitational acceleration	V, F	C, F, P	$\mathcal{U}(1, 5) 9.807 \times 10^0$
I.41.16	$L_{\text{rad}} = \frac{h}{2\pi} \frac{\omega^3}{\pi^2 c^2 (\exp(h\omega/2\pi kT) - 1)}$	x	Height	V, F	V, F, P	$\mathcal{U}(1, 5) \mathcal{U}_{\log}(10^{-2}, 10^0)$
		k	Boltzmann constant	V, F	C, F, P	$\mathcal{U}(1, 5) 1.381 \times 10^{-23}$
		T	Temperature	V, F	V, F, P	$\mathcal{U}(1, 5) \mathcal{U}_{\log}(10^1, 10^3)$
		L_{rad}	Radiation per frequency	V, F	V, F, P	N/A
I.44.4	$Q = nkT \ln(\frac{V_2}{V_1})$	h	Planck constant	V, F	C, F, P	$\mathcal{U}(1, 5) 6.626 \times 10^{-34}$
		ω	Frequency of electromagnetic wave	V, F	V, F, P	$\mathcal{U}(1, 5) \mathcal{U}_{\log}(10^{-1}, 10^1)$
		c	Speed of light	V, F	C, F, P	$\mathcal{U}(1, 5) 2.998 \times 10^8$
		k	Boltzmann constant	V, F	C, F, P	$\mathcal{U}(1, 5) 1.381 \times 10^{-23}$
I.50.26	$x = K (\cos \omega t + \epsilon \cos^2 \omega t)$	T	Temperature	V, F	V, F, P	$\mathcal{U}(1, 5) \mathcal{U}_{\log}(10^1, 10^3)$
		V_2	Volume	V, F	V, F, P	$\mathcal{U}(1, 5) \mathcal{U}_{\log}(10^{-5}, 10^{-3})$
		V_1	Volume	V, F	V, F, P	$\mathcal{U}(1, 5) \mathcal{U}_{\log}(10^{-5}, 10^{-3})$
		x	Amplitude	V, F	V, F	N/A
II.6.15a	$E = \frac{p}{4\pi\epsilon} \frac{3z}{r^5} \sqrt{x^2 + y^2}$	K	Amplitude	V, F	V, F, P	$\mathcal{U}(1, 3) \mathcal{U}_{\log}(10^{-1}, 10^1)$
		ω	Angular velocity	V, F	V, F	$\mathcal{U}(1, 3) \mathcal{U}_{\log}(10^1, 10^3)$
		t	Time	V, F	V, F, NN	$\mathcal{U}(1, 3) \mathcal{U}_{\log}(10^{-3}, 10^{-1})$
		ϵ	Variable	V, F	V, F	$\mathcal{U}(1, 3) \mathcal{U}_{\log}(10^{-3}, 10^{-1})$
II.6.15b	$E = \frac{p}{4\pi\epsilon} \frac{3 \cos \theta \sin \theta}{r^3}$	E	Electric field	V, F	V, F	N/A
		p	Electric dipole moment	V, F	V, F	$\mathcal{U}(1, 3) \mathcal{U}_{\log}(10^{-22}, 10^{-20})$
		ϵ	Vacuum permittivity	V, F	C, F, P	$\mathcal{U}(1, 3) 8.854 \times 10^{-12}$
		z	Position	V, F	V, F	$\mathcal{U}(1, 3) \mathcal{U}_{\log}(10^{-10}, 10^{-8})$
II.11.17	$n = n_0 \left(1 + \frac{p_0 E \cos \theta}{kT}\right)$	r	Distance	V, F	V, F, P	$\mathcal{U}(1, 3) \mathcal{U}_{\log}(10^{-10}, 10^{-8})$
		x	Position	V, F	V, F	$\mathcal{U}(1, 3) \mathcal{U}_{\log}(10^{-10}, 10^{-8})$
		y	Position	V, F	V, F	$\mathcal{U}(1, 3) \mathcal{U}_{\log}(10^{-10}, 10^{-8})$
		E	Electric field	V, F	V, F	N/A
II.11.20	$P = \frac{n_0 p_0^2 E}{3kT}$	p	Electric dipole moment	V, F	V, F	$\mathcal{U}(1, 3) \mathcal{U}_{\log}(10^{-22}, 10^{-20})$
		ϵ	Vacuum permittivity	V, F	C, F, P	$\mathcal{U}(1, 3) 8.854 \times 10^{-12}$
		θ	Angle	V, F	V, F	$\mathcal{U}(1, 3) \mathcal{U}(0, \pi)$
		r	Distance	V, F	V, F, P	$\mathcal{U}(1, 3) \mathcal{U}_{\log}(10^{-10}, 10^{-8})$
II.11.17	$n = n_0 \left(1 + \frac{p_0 E \cos \theta}{kT}\right)$	n	Number of polar molecules per angle per unit volume	V, F	V, F	N/A
		n_0	Number of molecules per unit volume	V, F	V, F, P	$\mathcal{U}(1, 3) \mathcal{U}_{\log}(10^{27}, 10^{29})$
		p_0	Electric dipole moment	V, F	V, F	$\mathcal{U}(1, 3) \mathcal{U}_{\log}(10^{-22}, 10^{-20})$
		E	Magnitude of electric field	V, F	V, F	$\mathcal{U}(1, 3) \mathcal{U}_{\log}(10^1, 10^3)$
II.11.20	$P = \frac{n_0 p_0^2 E}{3kT}$	θ	Angle	V, F	V, F, NN	$\mathcal{U}(1, 3) \mathcal{U}(0, 2\pi)$
		k	Boltzmann constant	V, F	C, F, P	$\mathcal{U}(1, 3) 1.381 \times 10^{-23}$
		T	Temperature	V, F	V, F, P	$\mathcal{U}(1, 3) \mathcal{U}_{\log}(10^1, 10^3)$
		P	Polarizability	V, F	V, F	N/A
II.11.20	$P = \frac{n_0 p_0^2 E}{3kT}$	n_0	Number of atom	V, F	V, I*, P	$\mathcal{U}(1, 5) \mathcal{U}_{\log}(10^{23}, 10^{25})$
		p_0	Electric dipole moment	V, F	V, F	$\mathcal{U}(1, 5) \mathcal{U}_{\log}(10^{-22}, 10^{-20})$
		E	Magnitude of electric field	V, F	V, F	$\mathcal{U}(1, 5) \mathcal{U}_{\log}(10^1, 10^3)$
		k	Boltzmann constant	V, F	C, F, P	$\mathcal{U}(1, 5) 1.381 \times 10^{-23}$
II.11.20	$P = \frac{n_0 p_0^2 E}{3kT}$	T	Temperature	V, F	V, F, P	$\mathcal{U}(1, 5) \mathcal{U}_{\log}(10^1, 10^3)$

Table S9: Hard set of our proposed datasets (part 3).

Eq. ID	Formula	Symbols	Properties		Distributions	
			Original	Ours	Original	Ours
II.11.27	$P = \frac{N\alpha}{1-(n\alpha/3)} \epsilon E$	P	Polarizability	V, F	V, F	N/A
		N	Number of atom	V, F	V, I*, P	$\mathcal{U}(0, 1)$ $\mathcal{U}_{\log}(10^{23}, 10^{25})$
		α	Molecular polarizability	V, F	V, F, P	$\mathcal{U}(0, 1)$ $\mathcal{U}_{\log}(10^{-33}, 10^{-31})$
		ϵ	Vacuum permittivity	V, F	C, F, P	$\mathcal{U}(1, 2)$ 8.854×10^{-12}
		E	Magnitude of electric field	V, F	V, F, P	$\mathcal{U}(1, 2)$ $\mathcal{U}_{\log}(10^1, 10^3)$
II.11.28	$\kappa = 1 + \frac{N\alpha}{1-(N\alpha/3)}$	κ	Electric dipole moment per unit volume	V, F	V, F	N/A
		N	Number of electric dipoles	V, F	V, I*, P	$\mathcal{U}(0, 1)$ $\mathcal{U}_{\log}(10^{23}, 10^{25})$
		α	Molecular polarizability	V, F	V, F, P	$\mathcal{U}(0, 1)$ $\mathcal{U}_{\log}(10^{-33}, 10^{-31})$
II.13.23	$\rho = \frac{\rho_0}{\sqrt{1-v^2/c^2}}$	ρ	Electric charge density	V, F	V, F, P	N/A
		ρ_0	Electric charge density	V, F	V, F, P	$\mathcal{U}(1, 5)$ $\mathcal{U}_{\log}(10^{27}, 10^{29})$
		v	Velocity	V, F	V, F, P	$\mathcal{U}(1, 2)$ $\mathcal{U}_{\log}(10^6, 10^8)$
		c	Speed of light	V, F	C, F, P	$\mathcal{U}(3, 10)$ 2.998×10^8
II.13.34	$j = \frac{\rho_0 v}{\sqrt{1-v^2/c^2}}$	j	Electric current	V, F	V, F	N/A
		ρ_0	Electric charge density	V, F	V, F, P	$\mathcal{U}(1, 5)$ $\mathcal{U}_{\log}(10^{27}, 10^{29})$
		v	Velocity	V, F	V, F, P	$\mathcal{U}(1, 2)$ $\mathcal{U}_{\log}(10^6, 10^8)$
		c	Speed of light	V, F	C, F, P	$\mathcal{U}(3, 10)$ 2.998×10^8
II.24.17	$k = \sqrt{\omega^2/c^2 - \pi^2/a^2}$	k	Wavenumber	V, F	V, F, P	N/A
		ω	Angular velocity	V, F	V, F	$\mathcal{U}(4, 6)$ $\mathcal{U}_{\log}(10^9, 10^{11})$
		c	Speed of light	V, F	C, F, P	$\mathcal{U}(1, 2)$ 2.998×10^8
		a	Length	V, F	V, F, P	$\mathcal{U}(2, 4)$ $\mathcal{U}_{\log}(10^{-3}, 10^{-1})$
II.35.18	$a = \frac{N}{\exp(\mu B/kT) + \exp(-\mu B/kT)}$	a	Number of atoms with the equivalent magnetic moment	V, F	V, I*, P	N/A
		N	Number of atoms per unit volume	V, F	V, I*, P	$\mathcal{U}(1, 3)$ $\mathcal{U}_{\log}(10^{23}, 10^{25})$
		μ	Magnetic moment	V, F	V, F, P	$\mathcal{U}(1, 3)$ $\mathcal{U}_{\log}(10^{-25}, 10^{-23})$
		B	Magnetic flux density	V, F	V, F, P	$\mathcal{U}(1, 3)$ $\mathcal{U}_{\log}(10^{-3}, 10^{-1})$
		k	Boltzmann constant	V, F	C, F, P	$\mathcal{U}(1, 3)$ 1.381×10^{-23}
		T	Temperature	V, F	V, F, P	$\mathcal{U}(1, 3)$ $\mathcal{U}_{\log}(10^1, 10^3)$
II.35.21	$M = N\mu \tanh\left(\frac{\mu B}{kT}\right)$	M	Number of magnetized atoms	V, F	V, I*, P	N/A
		N	Number of atom	V, F	V, I*, P	$\mathcal{U}(1, 5)$ $\mathcal{U}_{\log}(10^{23}, 10^{25})$
		μ	Magnetic moment	V, F	V, F, P	$\mathcal{U}(1, 5)$ $\mathcal{U}_{\log}(10^{-25}, 10^{-23})$
		B	Magnetic flux density	V, F	V, F, P	$\mathcal{U}(1, 5)$ $\mathcal{U}_{\log}(10^{-3}, 10^{-1})$
		T	Boltzmann constant	V, F	C, F, P	$\mathcal{U}(1, 5)$ 1.381×10^{-23}
II.36.38	$x = \frac{\mu H}{kT} + \frac{\mu \lambda}{\epsilon c^2 kT} M$	x	Parameter of magnetization	V, F	V, F	N/A
		μ	Magnetic moment	V, F	V, F	$\mathcal{U}(1, 3)$ $\mathcal{U}_{\log}(10^{-25}, 10^{-23})$
		H	Magnetic field strength	V, F	V, F	$\mathcal{U}(1, 3)$ $\mathcal{U}_{\log}(10^{-3}, 10^{-1})$
		k	Boltzmann constant	V, F	C, F, P	$\mathcal{U}(1, 3)$ 1.381×10^{-23}
		T	Temperature	V, F	V, F, P	$\mathcal{U}(1, 3)$ $\mathcal{U}_{\log}(10^1, 10^3)$
		λ	Constant	V, F	V, F, NN	$\mathcal{U}(1, 3)$ $\mathcal{U}(0, 1)$
		ϵ	Vacuum permittivity	V, F	C, F, P	$\mathcal{U}(1, 3)$ 8.854×10^{-12}
		c	Speed of light	V, F	C, F, P	$\mathcal{U}(1, 3)$ 2.998×10^8
III.4.33	$E = \frac{\hbar\omega}{2\pi(\exp(\hbar\omega/2\pi kT)-1)}$	M	Number of magnetized atoms	V, F	V, I*, P	$\mathcal{U}(1, 3)$ $\mathcal{U}_{\log}(10^{23}, 10^{25})$
		E	Energy	V, F	V, F, P	N/A
		h	Planck constant	V, F	C, F, P	$\mathcal{U}(1, 5)$ 6.626×10^{-34}
		ω	Frequency	V, F	V, F, P	$\mathcal{U}(1, 5)$ $\mathcal{U}_{\log}(10^8, 10^{10})$
		k	Boltzmann constant	V, F	C, F, P	$\mathcal{U}(1, 5)$ 1.381×10^{-23}
III.9.52	$P_{\text{I}\rightarrow\text{II}} = \left(\frac{2\pi\mu Et}{h}\right)^2 \frac{\sin^2((\omega - \omega_0)t/2)}{(\omega - \omega_0)t/2}$	T	Temperature	V, F	V, F, P	$\mathcal{U}(1, 5)$ $\mathcal{U}_{\log}(10^1, 10^3)$
		$P_{\text{I}\rightarrow\text{II}}$	Probability	V, F	V, F, NN	N/A
		μ	Electric dipole moment	V, F	V, F	$\mathcal{U}(1, 3)$ $\mathcal{U}_{\log}(10^{-22}, 10^{-20})$
		E	Magnitude of electric field	V, F	V, F	$\mathcal{U}(1, 3)$ $\mathcal{U}_{\log}(10^1, 10^3)$
		t	Time	V, F	V, F, NN	$\mathcal{U}(1, 3)$ $\mathcal{U}_{\log}(10^{-18}, 10^{-16})$
		h	Planck constant	V, F	C, F, P	$\mathcal{U}(1, 3)$ 6.626×10^{-34}
		ω	Frequency	V, F	V, F, P	$\mathcal{U}(1, 5)$ $\mathcal{U}_{\log}(10^8, 10^{10})$
		ω_0	Resonant frequency	V, F	V, F, P	$\mathcal{U}(1, 5)$ $\mathcal{U}_{\log}(10^8, 10^{10})$

Table S10: Hard set of our proposed datasets (part 4).

Eq. ID	Formula	Symbols	Properties		Distributions	
			Original	Ours	Original	Ours
III.10.19	$E = \mu \sqrt{B_x^2 + B_y^2 + B_z^2}$	E Energy	V, F	V, F	N/A	N/A
		μ Magnetic moment	V, F	V, F	$\mathcal{U}(1, 5)$	$\mathcal{U}_{\log}(10^{-25}, 10^{-23})$
		B_x Element of magnetic field	V, F	V, F	$\mathcal{U}(1, 5)$	$\mathcal{U}_{\log}(10^{-3}, 10^{-1})$
		B_y Element of magnetic field	V, F	V, F	$\mathcal{U}(1, 5)$	$\mathcal{U}_{\log}(10^{-3}, 10^{-1})$
III.21.20	$J = -\rho \frac{q}{m} A$	B_z Element of magnetic field	V, F	V, F	$\mathcal{U}(1, 5)$	$\mathcal{U}_{\log}(10^{-3}, 10^{-1})$
		J Electric Current	V, F	V, F	N/A	N/A
		ρ Electric charge density	V, F	V, F, N	$\mathcal{U}(1, 5)$	$\mathcal{U}_{\log}(10^{27}, 10^{29})$
		q Electric charge	V, F	V, F, N	$\mathcal{U}(1, 5)$	$\mathcal{U}_{\log}(10^{-11}, 10^{-9})$
B1	$A = \left(\frac{Z_1 Z_2 \alpha \hbar c}{4E \sin^2(\theta/2)} \right)^2$	A Magnetic vector potential	V, F	V, F	$\mathcal{U}(1, 5)$	$\mathcal{U}_{\log}(10^{-3}, 10^{-1})$
		m Mass	V, F	V, F, P	$\mathcal{U}(1, 5)$	$\mathcal{U}_{\log}(10^{-30}, 10^{-28})$
		A Differential scattering cross section	V, F	V, F	N/A	N/A
		Z_1 Atomic number	V, F	V, I, P	$\mathcal{U}(1, 2)$	$\mathcal{U}_{\log}(10^0, 10^1)$
B2	$k = \frac{mk_G}{L^2}$ $\left(1 + \sqrt{1 + \frac{2EL^2}{mk_G^2}} \cos(\theta_1 - \theta_2) \right)$	Z_2 Atomic number	V, F	V, I, P	$\mathcal{U}(1, 2)$	$\mathcal{U}_{\log}(10^0, 10^1)$
		α Fine structure constant	V, F	C, F, P	$\mathcal{U}(1, 5)$	7.297×10^{-3}
		h Dirac's constant	V, F	C, F, P	$\mathcal{U}(1, 2)$	1.055×10^{-34}
		c Speed of light	V, F	C, F, P	$\mathcal{U}(1, 2)$	2.998×10^8
B3	$r = \frac{d(1-\alpha^2)}{1+\alpha \cos(\theta_1-\theta_2)}$	E Non-relativistic kinetic energy	V, F	V, F, P	$\mathcal{U}(1, 3)$	$\mathcal{U}_{\log}(10^{-18}, 10^{-16})$
		θ Scattering angle	V, F	V, F, NN	$\mathcal{U}(1, 3)$	$\mathcal{U}(0, 2\pi)$
		k Variable	V, F	V, F	N/A	N/A
		m Mass (The Earth)	V, F	V, F, P	$\mathcal{U}(1, 3)$	$\mathcal{U}_{\log}(10^{23}, 10^{25})$
B4	$v = \sqrt{\frac{2}{m} \left(E - U - \frac{L^2}{2mr^2} \right)}$	k_G Variable	V, F	V, F, P	$\mathcal{U}(1, 3)$	$\mathcal{U}_{\log}(10^9, 10^{11})$
		L Distance	V, F	V, F, P	$\mathcal{U}(1, 3)$	$\mathcal{U}_{\log}(10^8, 10^{10})$
		E Energy	V, F	V, F, P	$\mathcal{U}(1, 3)$	$\mathcal{U}_{\log}(10^{25}, 10^{27})$
		θ_1 Angle	V, F	V, F, NN	$\mathcal{U}(0, 6)$	$\mathcal{U}(0, 2\pi)$
B5	$t = \frac{2\pi d^{3/2}}{\sqrt{G(m_1+m_2)}}$	θ_2 Angle	V, F	V, F, NN	$\mathcal{U}(0, 6)$	$\mathcal{U}(0, 2\pi)$
		r Distance	V, F	V, F, P	N/A	N/A
		v Velocity	V, F	V, F, P	N/A	N/A
		m Mass (The Earth)	V, F	V, F, P	$\mathcal{U}(1, 3)$	$\mathcal{U}_{\log}(10^{23}, 10^{25})$
B6	$\alpha = \sqrt{1 + \frac{2\epsilon^2 EL^2}{m(Z_1 Z_2 q^2)^2}}$	E Energy	V, F	V, F, P	$\mathcal{U}(8, 12)$	$\mathcal{U}_{\log}(10^{25}, 10^{27})$
		U Potential energy	V, F	V, F, P	$\mathcal{U}(1, 3)$	$\mathcal{U}_{\log}(10^{25}, 10^{27})$
		L Angular momentum	V, F	V, F	$\mathcal{U}(1, 3)$	$\mathcal{U}_{\log}(10^8, 10^{10})$
		r Distance	V, F	V, F, P	$\mathcal{U}(1, 3)$	$\mathcal{U}_{\log}(10^8, 10^{10})$
B7	$H = \sqrt{\frac{8\pi G\rho}{3} - \frac{k_f c^2}{a_f^2}}$	t Orbital period	V, F	V, F, P	N/A	N/A
		d Semimajor axis of elliptical orbit	V, F	V, F, P	$\mathcal{U}(1, 3)$	$\mathcal{U}_{\log}(10^8, 10^{10})$
		G Gravitational constant	V, F	C, F, P	$\mathcal{U}(1, 3)$	6.674×10^{-11}
		m_1 Mass (The Earth)	V, F	V, F, P	$\mathcal{U}(1, 3)$	$\mathcal{U}_{\log}(10^{23}, 10^{25})$
B8	$P = -\frac{32}{5} \frac{G^4}{c^5} \frac{(m_1 m_2)^2 (m_1 + m_2)}{r^5}$	m_2 Mass	V, F	V, F, P	$\mathcal{U}(1, 3)$	$\mathcal{U}_{\log}(10^{23}, 10^{25})$
		q Electric charge	V, F	V, F	$\mathcal{U}(1, 3)$	$\mathcal{U}_{\log}(10^{-11}, 10^{-9})$
		H Hubble's constant	V, F	V, F, P	N/A	N/A
		G Gravitational constant	V, F	C, F, P	$\mathcal{U}(1, 3)$	6.674×10^{-11}
B9	$P = -\frac{32}{5} \frac{G^4}{c^5} \frac{(m_1 m_2)^2 (m_1 + m_2)}{r^5}$	ρ Density of the Universe	V, F	V, F, P	$\mathcal{U}(1, 3)$	$\mathcal{U}_{\log}(10^{-27}, 10^{-25})$
		k_f Spacetime curvature	V, F	V, I	$\mathcal{U}(1, 2)$	$\mathcal{U}(-1, 1)$
		c Speed of light	V, F	C, F, P	$\mathcal{U}(1, 2)$	2.998×10^8
		a_f Radius	V, F	V, F, P	$\mathcal{U}(1, 3)$	$\mathcal{U}_{\log}(10^8, 10^{10})$
B10	$P = -\frac{32}{5} \frac{G^4}{c^5} \frac{(m_1 m_2)^2 (m_1 + m_2)}{r^5}$	P Gravitational wave energy	V, F	V, F	N/A	N/A
		G Gravitational constant	V, F	C, F, P	$\mathcal{U}(1, 2)$	6.674×10^{-11}
		c Speed of light	V, F	C, F, P	$\mathcal{U}(1, 2)$	2.998×10^8
		m_1 Mass	V, F	V, F, P	$\mathcal{U}(1, 5)$	$\mathcal{U}_{\log}(10^{23}, 10^{25})$
B11	$P = -\frac{32}{5} \frac{G^4}{c^5} \frac{(m_1 m_2)^2 (m_1 + m_2)}{r^5}$	m_2 Mass	V, F	V, F, P	$\mathcal{U}(1, 5)$	$\mathcal{U}_{\log}(10^{23}, 10^{25})$
		r Distance	V, F	V, F, P	$\mathcal{U}(1, 2)$	$\mathcal{U}_{\log}(10^8, 10^{10})$

Table S11: Hard set of our proposed datasets (part 5).

Eq. ID	Formula	Symbols	Properties		Distributions	
			Original	Ours	Original	Ours
B10	$\cos \theta_1 = \frac{\cos \theta_2 - v/c}{(1-v/c) \cos \theta_2}$	$\cos \theta_1$ Value	V, F	V, F	N/A	N/A
		θ_2 Angle	V, F	V, F	$\mathcal{U}(1, 3)$	$\mathcal{U}(0, 2\pi)$
		v Velocity	V, F	V, F	$\mathcal{U}(1, 3)$	$\mathcal{U}_{\log}(10^5, 10^7)$
		c Speed of light	V, F	C, F, P	$\mathcal{U}(4, 6)$	2.998×10^8
B11	$I = I_0 \left(\frac{\sin(\alpha/2)}{\alpha/2} \frac{\sin(N\delta/2)}{\sin(\delta/2)} \right)^2$	I Wave intensity	V, F	V, F, P	N/A	N/A
		I_0 Amplitude of wave	V, F	V, F, P	$\mathcal{U}(1, 3)$	$\mathcal{U}_{\log}(10^{-3}, 10^{-1})$
		α Wavelength of X-ray	V, F	V, F, P	$\mathcal{U}(1, 3)$	$\mathcal{U}_{\log}(10^{-11}, 10^{-9})$
		N Number of phase difference	V, F	V, I, P	$\mathcal{U}(1, 2)$	$\mathcal{U}_{\log}(10^0, 10^2)$
B12	$F = \frac{q}{4\pi\epsilon y^2}$ $\left(4\pi\epsilon V_e d - \frac{qdy^3}{(y^2 - d^2)^2} \right)$	δ Wavelength of X-ray	V, F	V, F, P	$\mathcal{U}(1, 3)$	$\mathcal{U}_{\log}(10^{-11}, 10^{-9})$
		F Force	V, F	V, F	N/A	N/A
		q Electric charge	V, F	V, F	$\mathcal{U}(1, 5)$	$\mathcal{U}_{\log}(10^{-3}, 10^{-1})$
		ϵ Vacuum permittivity	V, F	C, F, P	$\mathcal{U}(1, 5)$	8.854×10^{-12}
		y Distance	V, F	V, F, P	$\mathcal{U}(1, 3)$	$\mathcal{U}_{\log}(10^{-2}, 10^0)$
		V_e Voltage	V, F	V, F	$\mathcal{U}(1, 5)$	$\mathcal{U}_{\log}(10^{-1}, 10^1)$
B13	$V_e = \frac{q}{4\pi\epsilon\sqrt{r^2 + d^2 - 2dr \cos \alpha}}$	d Distance	V, F	V, F, P	$\mathcal{U}(4, 6)$	$\mathcal{U}_{\log}(10^{-2}, 10^0)$
		V_e Potential	V, F	V, F	N/A	N/A
		ϵ permittivity	V, F	V, F, P	$\mathcal{U}(1, 5)$	$\mathcal{U}_{\log}(10^{-12}, 10^{-10})$
		q Electric charge	V, F	V, F	$\mathcal{U}(1, 5)$	$\mathcal{U}_{\log}(10^{-3}, 10^{-1})$
		r Distance	V, F	V, F, P	$\mathcal{U}(1, 3)$	$\mathcal{U}_{\log}(10^{-2}, 10^0)$
B14	$V_e = E_f \cos \theta \left(\frac{\alpha-1}{\alpha+2} \frac{d^3}{r^2} - r \right)$	d Distance between dipoles	V, F	V, F, P	$\mathcal{U}(4, 6)$	$\mathcal{U}_{\log}(10^{-2}, 10^0)$
		α Angle	V, F	V, F	$\mathcal{U}(0, 6)$	$\mathcal{U}(0, 2\pi)$
		V_e Potential (out)	V, F	V, F	N/A	N/A
		E_f Magnitude of electric field	V, F	V, F	$\mathcal{U}(1, 5)$	$\mathcal{U}_{\log}(10^1, 10^3)$
		θ Angle	V, F	V, F	$\mathcal{U}(0, 6)$	$\mathcal{U}(0, 2\pi)$
B15	$\omega_0 = \frac{\sqrt{1 - \frac{v^2}{c^2}}}{1 + \frac{v}{c} \cos \theta} \omega$	r Distance	V, F	V, F, P	$\mathcal{U}(1, 5)$	$\mathcal{U}_{\log}(10^{-2}, 10^0)$
		d Radius of dielectric sphere	V, F	V, F, P	$\mathcal{U}(1, 5)$	$\mathcal{U}_{\log}(10^{-2}, 10^0)$
		α Polarizability	V, F	V, F	$\mathcal{U}(1, 5)$	$\mathcal{U}_{\log}(10^{-1}, 10^1)$
		ω_0 Frequency of electromagnetic waves	V, F	V, F	N/A	N/A
		v Velocity	V, F	V, F, P	$\mathcal{U}(1, 3)$	$\mathcal{U}_{\log}(10^5, 10^7)$
B16	$E = qV_e + \sqrt{(p - qA)^2 c^2 + m^2 c^4}$	c Speed of light	V, F	C, F, P	$\mathcal{U}(5, 20)$	2.998×10^8
		ω Frequency of electromagnetic waves	V, F	V, F, P	$\mathcal{U}(1, 5)$	$\mathcal{U}_{\log}(10^9, 10^{11})$
		θ Angle	V, F	V, F	$\mathcal{U}(0, 6)$	$\mathcal{U}(0, 2\pi)$
		E Energy	V, F	V, F	N/A	N/A
		p Momentum	V, F	V, F	$\mathcal{U}(1, 5)$	$\mathcal{U}_{\log}(10^{-9}, 10^{-7})$
		q Electric charge	V, F	V, F	$\mathcal{U}(1, 5)$	$\mathcal{U}_{\log}(10^{-11}, 10^{-9})$
B17	$E = \frac{1}{2m} \left(p^2 + m^2 \omega^2 x^2 \left(1 + \alpha \frac{x}{y} \right) \right)$	A Vector potential	V, F	V, F	$\mathcal{U}(1, 5)$	$\mathcal{U}_{\log}(10^1, 10^3)$
		c Speed of light	V, F	C, F, P	$\mathcal{U}(1, 5)$	2.998×10^8
		m Mass	V, F	V, F, P	$\mathcal{U}(1, 5)$	$\mathcal{U}_{\log}(10^{-30}, 10^{-28})$
		V_e Voltage	V, F	V, F	$\mathcal{U}(1, 5)$	$\mathcal{U}_{\log}(10^{-1}, 10^1)$
		E Energy	V, F	V, F	N/A	N/A
		m Mass	V, F	V, F, P	$\mathcal{U}(1, 5)$	$\mathcal{U}_{\log}(10^{-30}, 10^{-28})$
B18	$p_f = -\frac{1}{8\pi G}$ $\left(\frac{c^4 k_f}{a_f^2} + c^2 H^2 (1 - 2\alpha) \right)$	p Momentum	V, F	V, F	$\mathcal{U}(1, 5)$	$\mathcal{U}_{\log}(10^{-9}, 10^{-7})$
		ω Frequency of electromagnetic waves	V, F	V, F, P	$\mathcal{U}(1, 5)$	$\mathcal{U}_{\log}(10^9, 10^{11})$
		x Position	V, F	V, F	$\mathcal{U}(1, 5)$	$\mathcal{U}_{\log}(10^{-11}, 10^{-9})$
		α Deviation from the harmonic oscillator	V, F	V, F	$\mathcal{U}(1, 5)$	$\mathcal{U}_{\log}(10^{-1}, 10^1)$
		y Distance	V, F	V, F, P	$\mathcal{U}(1, 5)$	$\mathcal{U}_{\log}(10^{-11}, 10^{-9})$
		p_f Pressure	V, F	V, F	N/A	N/A
B19	$G = \frac{1}{8\pi G}$ $\left(\frac{c^4 k_f}{a_f^2} + c^2 H^2 (1 - 2\alpha) \right)$	G Gravitational constant	V, F	C, F, P	$\mathcal{U}(1, 5)$	6.674×10^{-11}
		c Speed of light	V, F	C, F, P	$\mathcal{U}(1, 5)$	2.998×10^8
		k_f Variable	V, F	V, F	$\mathcal{U}(1, 5)$	$\mathcal{U}_{\log}(10^1, 10^3)$
		a_f Distance	V, F	V, F, P	$\mathcal{U}(1, 5)$	$\mathcal{U}_{\log}(10^8, 10^{10})$
		H Variable	V, F	V, F, P	$\mathcal{U}(1, 5)$	$\mathcal{U}_{\log}(10^0, 10^2)$
		α Variable	V, F	V, F	$\mathcal{U}(1, 5)$	$\mathcal{U}(-10, 10)$
B20	$A = \frac{\alpha^2 h^2}{4\pi m^2 c^2} \left(\frac{\omega_0}{\omega} \right)^2$ $\left(\frac{\omega_0}{\omega} + \frac{\omega}{\omega_0} - \sin^2 \theta \right)$	A Differential cross section	V, F	V, F	N/A	N/A
		α Fine structure constant	V, F	C, F, P	$\mathcal{U}(1, 5)$	7.297×10^{-3}
		h Planck constant	V, F	C, F, P	$\mathcal{U}(1, 5)$	6.626×10^{-34}
		m Electron mass	V, F	C, F, P	$\mathcal{U}(1, 5)$	9.109×10^{-31}
		c Speed of light	V, F	C, F, P	$\mathcal{U}(1, 5)$	2.998×10^8
		ω_0 Frequency	V, F	V, F, P	$\mathcal{U}(1, 5)$	$\mathcal{U}_{\log}(10^9, 10^{11})$
		ω Frequency	V, F	V, F, P	$\mathcal{U}(1, 5)$	$\mathcal{U}_{\log}(10^9, 10^{11})$
		θ Scattering angle	V, F	V, F	$\mathcal{U}(0, 6)$	$\mathcal{U}(0, 2\pi)$

B Hyperparameters for Five Existing SR Baselines

Table S12 shows the hyperparameter space for the five existing symbolic regression baselines. The hyperparameters of gplearn [22]¹², AFP [43], and AFP-FE [42]¹³ are optimized by Optuna [2], a hyperparameter optimization framework.

Table S12: Hyperparameter sets for the five existing symbolic regression baselines.

Method	Hyperparameter sets
gplearn	100 trials with random combinations of the following hyperparameter spaces: $population_size: \mathcal{U}(10^2, 10^3)$, $generations: \mathcal{U}(10, 10^2)$, $stopping_criteria: \mathcal{U}(10^{-10}, 10^{-2})$, $warm_start: \{\text{True, False}\}$, $const_range: \{\text{None, } (-1.0, 1.0), (-10, 10), (-10^2, 10^2), (-10^3, 10^3), (-10^4, 10^4)\}$, $max_samples: \mathcal{U}(0.9, 1.0)$, $parsimony_coefficient: \mathcal{U}(10^{-3}, 10^{-2})$
AFP	100 trials with random combinations of the following hyperparameter spaces: $popsize: \mathcal{U}(100, 1000)$, $g: \mathcal{U}(250, 2500)$, $stop_threshold: \mathcal{U}(10^{-10}, 10^{-2})$, $op_list: \{['n', 'v', '+', '-', '*', '/', 'exp', 'log', '2', '3', 'sqrt'],$ $['n', 'v', '+', '-', '*', '/', 'exp', 'log', '2', '3', 'sqrt', 'sin', 'cos']\}$
AFP-FE	100 trials with random combinations of the following hyperparameter spaces: $popsize: \mathcal{U}(100, 1000)$, $g: \mathcal{U}(250, 2500)$, $stop_threshold: \mathcal{U}(10^{-10}, 10^{-2})$, $op_list: \{['n', 'v', '+', '-', '*', '/', 'exp', 'log', '2', '3', 'sqrt'],$ $['n', 'v', '+', '-', '*', '/', 'exp', 'log', '2', '3', 'sqrt', 'sin', 'cos']\}$
AI Feynman	$\{bftt: 60, epoch: 300, op: '7ops.txt', poly_deg: 3\}$, $\{bftt: 60, epoch: 300, op: '10ops.txt', poly_deg: 3\}$, $\{bftt: 60, epoch: 300, op: '14ops.txt', poly_deg: 3\}$, $\{bftt: 60, epoch: 300, op: '19ops.txt', poly_deg: 3\}$, $\{bftt: 120, epoch: 300, op: '14ops.txt', poly_deg: 4\}$, $\{bftt: 120, epoch: 300, op: '19ops.txt', poly_deg: 4\}$, $\{bftt: 60, epoch: 500, op: '7ops.txt', poly_deg: 3\}$, $\{bftt: 60, epoch: 500, op: '10ops.txt', poly_deg: 3\}$, $\{bftt: 60, epoch: 500, op: '14ops.txt', poly_deg: 3\}$, $\{bftt: 60, epoch: 500, op: '19ops.txt', poly_deg: 3\}$
DSR	$\{seed: 1, function_set: ['add', 'sub', 'mul', 'div', 'sin', 'cos', 'exp', 'log']\}$, $\{seed: 2, function_set: ['add', 'sub', 'mul', 'div', 'sin', 'cos', 'exp', 'log']\}$, $\{seed: 3, function_set: ['add', 'sub', 'mul', 'div', 'sin', 'cos', 'exp', 'log']\}$, $\{seed: 4, function_set: ['add', 'sub', 'mul', 'div', 'sin', 'cos', 'exp', 'log']\}$, $\{seed: 5, function_set: ['add', 'sub', 'mul', 'div', 'sin', 'cos', 'exp', 'log']\}$, $\{seed: 1, function_set: ['add', 'sub', 'mul', 'div', 'sin', 'cos', 'exp', 'log', 'const']\}$, $\{seed: 2, function_set: ['add', 'sub', 'mul', 'div', 'sin', 'cos', 'exp', 'log', 'const']\}$, $\{seed: 3, function_set: ['add', 'sub', 'mul', 'div', 'sin', 'cos', 'exp', 'log', 'const']\}$, $\{seed: 4, function_set: ['add', 'sub', 'mul', 'div', 'sin', 'cos', 'exp', 'log', 'const']\}$, $\{seed: 5, function_set: ['add', 'sub', 'mul', 'div', 'sin', 'cos', 'exp', 'log', 'const']\}$

¹²<https://gplearn.readthedocs.io/en/stable/reference.html#symbolic-regressor>

¹³<https://github.com/cavalab/ellyn>

C Symbolic Transformer

In this section, we describe our Symbolic Transformer baseline and pretraining strategy, and discuss the degree of the test data leakage during the pretraining. We repeat that while the Symbolic Transformer itself is a new model, the main contribution of this work lies in the datasets and benchmark of symbolic regression for scientific discovery (SRSD). We also note that our Symbolic Transformer is not necessarily designed to show improvements over the existing Transformer-based symbolic regression models [4, 51] including contemporary work such as [18]. Our Transformer-based baseline is simply inspired by recent advances in deep learning, specifically Transformer-based high-performance, modern, and flexible models such as [8, 9, 52].

C.1 Architecture Design

A Symbolic Transformer is an encoder-decoder network to predict a binary equation tree corresponding to input tabular data points. The encoder inputs sampled tabular data from an equation and outputs variable-wise features. The decoder inputs them and outputs a preorder sequence of tokens in an autoregressive manner to build a binary equation tree.

First, we describe an encoder that inputs tabular data and outputs variable-wise features. The tabular data here have the following properties:

- Each row is a data point sampled from the expected equation
- Each column corresponds to the input variable of the equation (x_1, x_2, \dots) or the output of the equation (y).

For such data, the relation between the input tabular data and the output equation is desired to have the following properties:

- Permutation-invariant in each row; since there is no meaningful order between each sampled point, the output equation is expected not to change no matter how the rows are rearranged.
- Permutation-equivariant for each column and variable; when the columns of the input tabular data are rearranged, the order of variables in the output equation is expected to change corresponding to the input column. (e.g., assume the formula $y = x_1 - x_2$, if the x_1 column and the x_2 column of the input tabular data are swapped, the expected output is $y = x_2 - x_1$.)

To handle such permutation-invariant and permutation-equivariant data structures, the ideas of PointNet [6], which handles 3D point clouds, and Deep Sets [60], which handles set data, can be referred to. The approach proposed in these papers is to utilize point-wise transformation using Shared Multi Layer Perceptron (MLP) (permutation-equivariant operation) and aggregation using Pooling (permutation-invariant operation).

When applied to tabular data, a sample point-wise feature can be obtained by combining Shared MLP and column-wise (variable-wise) pooling. Similarly, a variable-wise feature can be obtained by combining Shared MLP and row-wise (sample point-wise) Pooling. In both operations, by aggregating once and then combining the features with the features of each cell (this idea is used in semantic segmentation network in PointNet [6]), it can be expected that the whole information of aggregated direction will propagate to each cell. We call this operation feature splatting. Note that it is a permutation-equivariant operation.

The proposed network architecture is shown in Fig. S1. The proposed encoder consists of two encoding blocks, each block consisting of 1.) Shared MLP, 2.) row-wise (sample point-wise) pooling, 3.) row-wise feature splatting, 4.) Shared MLP, 5.) column-wise (variable-wise) pooling, and 6.) column-wise feature splatting. The encoder is permutation-equivariant, and information of each cell propagates to both the row-axis and column-axis. Finally, row-wise (sample point-wise) pooling can obtain the variable-wise feature.

The decoder of our Symbolic Transformer is a Transformer decoder [52] that takes a variable-wise feature and a preorder sequence of tokens (to express the equation as a binary equation tree) as input and outputs the next token. The next token is estimated with Multi-head Attention over the variable-wise feature from the input tokens. During training, we use the teacher forcing method [58] and feed the first ($j - 1$) tokens in the ground-truth preorder sequence to the decoder for predicting

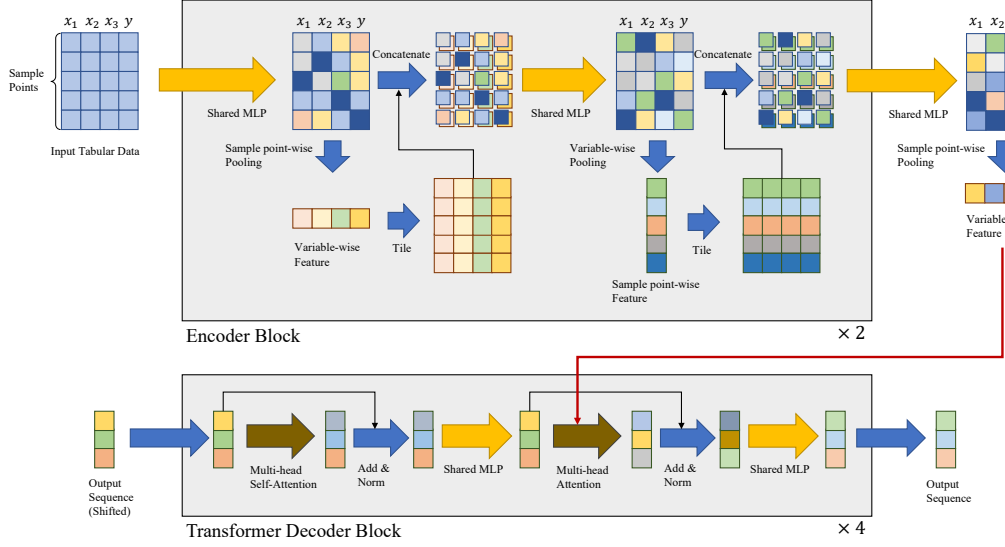


Figure S1: Architecture of Symbolic Transformer.

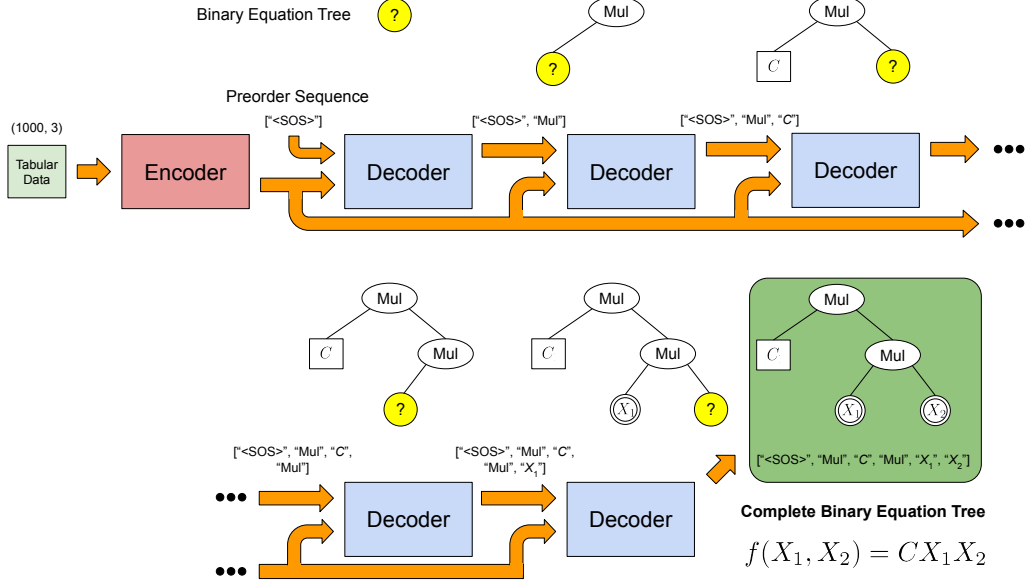


Figure S2: Illustration of Symbolic Transformer's inference process for given tabular data which consists of 1,000 samples. Each sample is a 3-dimensional vector whose first two and last values correspond to two variables and one target value, respectively. Yellow nodes indicate next tokens (nodes) to be predicted.

the next (j -th) token and computing cross-entropy loss with a scheduled sampling strategy [28]. During inference, the decoder predicts the next token autoregressively, using a sequence of previously-predicted tokens as input tokens as illustrated in Fig. S2. From the resulting preorder sequence of tokens, the binary equation tree is generated as the output of the Symbolic Transformer method.

For each training batch, we also mask next token candidates as the Symbolic Transformer model will know the potential maximum number of variables in the target equation from the shape of the

training batch. Suppose that a training batch consists of tabular data whose shape is $(1,000, 3)$ ¹⁴, the decoder should not predict three or more unique variable tokens as part of the preorder sequence.

It should be worth noting that when predicting the next token of a preorder sequence, we take advantage of properties of binary equation tree for efficient inference. Since we predict a preorder sequence to build a binary equation tree, we can terminate the inference of the next token when all the child nodes in the binary equation tree built from the resulting sequence expresses are tokens for either constant or variable symbols *i.e.*, the binary equation tree is complete and cannot be extend anymore, thus we can terminate the inference without predicting “<EOS>”, the end of sequence token used in standard seq2seq tasks [47].

C.2 Pretraining and Hyperparameters

Here, we describe our pretraining strategy for the Symbolic Transformer baseline. As described in Section C.1], the decoder of the Symbolic Transformer is trained to predict a next token of a preorder sequence to express the true binary equation tree, and thus requires both 1) a true sequence of the tokens and 2) tabular data (samples).

The 120 SRSD datasets proposed in this study, however, should not be directly used for pretraining the Symbolic Transformer baseline. Since the datasets are designed to assess the potential of symbolic regression methods towards scientific discovery, we cannot use the SRSD datasets for both pretraining and testing the Symbolic Transformer baseline. Otherwise, it will result in having the baseline method learn from the pairs of tabular data and true sequences during training session and test the method using tabular data from a similar distribution, which may be considered as test data leakage.

Moreover, pretraining datasets are usually significantly larger than the target datasets (which are the SRSD datasets in this study) [8, 9, 29]. To address the issues, we generated a large-scale set of synthesized datasets for pretraining the Symbolic Transformer baseline. Specifically, we built a bi-gram Naïve Bayes language model to generate preorder sequences of tokens that express binary equation trees like those in the SRSD datasets. Having randomly generated a target equation for pretraining, we randomly chose k for each of the variables in the equation independently to define its sampling range $\mathcal{U}_{\log}(10^{k-1}, 10^{k+1})$. Given a generated equation, we created up to 10 sets of tabular datasets with different sampling ranges we randomly chose as described above.

Using the approach, we generated 24,232 synthesized datasets. In the datasets, there are 4,501 generated equations, and 1,841 of them are unique sequences. We pretrained the Symbolic Transformer baseline on the synthesized datasets for three epochs, using the SGD optimizer and a linear learning rate scheduler with warmup (1,000 steps)¹⁵ where the initial learning rate and weight decay are 0.1 and 10^{-4} , respectively. A training batch at each step consists of 1,000 random samples from one of the synthesized datasets, and one epoch in this pretraining consists of 24,232 training steps. The Symbolic Transformer is implemented with PyTorch [39], and we implemented the pretraining and evaluation sessions, using torchdistill [33] for securing reproducibility of the experiments.

C.3 Are the test datasets leaked while pretraining Symbolic Transformer?

In terms of normalized edit distance we proposed, the Symbolic Transformer baseline performed the best among our baseline methods for the SRSD datasets as shown in Section 5.3. To achieve the results, the Symbolic Transformer baseline model took advantage of being pretrained on a large-scale set of synthesized datasets we generated (See Section C.2). From the performance gap between the Symbolic Transformer and the other baselines, it is reasonable to suspect that the test set of our SRSD datasets may be leaked during the pretraining step. Given a pair of a synthesized training dataset X_R and an SRSD test dataset X_S , we assess the degree of the leakage, following the two steps:

Step 1 Compute normalized edit distance (Eq. (3)) between the true equations in the two datasets.

Step 2 If the resulting normalized edit distance (Step 1) is zero, then compute intersection of union (IoU) between sampling domains of the datasets by Eq. (S1) for each input variable:

¹⁴The last (rightmost) column in input tabular data indicates the target values, thus should not be a input variable for the equation to be predicted.

¹⁵https://huggingface.co/docs/transformers/main_classes/optimizer_schedules#transformers.get_linear_schedule_with_warmup

$$\text{IoU}(X_R^i, X_S^i) = \frac{\max(\min(X_R^i), \min(X_S^i)) - \min(\max(X_R^i), \max(X_S^i))}{\min(\min(X_R^i), \min(X_S^i)) - \max(\max(X_R^i), \max(X_S^i))}, \quad (\text{S1})$$

where X_R^i and X_S^i are sets of sampled values in the i -th variable for the given synthesized training dataset and the SRSD test dataset, respectively.

Following the procedure above, we assess the degree of the leakage for all the combinations of 120 SRSD datasets versus 24,232 synthesized datasets for pretraining. We take equation-wise average of the IoU values and then compute the average IoU over the 120 equation-wise average IoU values. The resulting mean IoU is 0.00215, and the IoU defined in Eq. (S1) is designed to be normalized in range of 0 to 1. From the result, we conclude that there is no significant leakage from our SRSD datasets while pretraining the Symbolic Transformer.

D Qualitative Analysis

This section discusses qualitative analysis for the experimental results above.

Here we highlight some examples that the Symbolic Transformer baseline method perform better with respect to the normalized edit distance than other baselines and vice versa. Taking I.12.4 in Table 1 as an example, $E = \frac{q_1}{4\pi\epsilon r^2}$ is simplified by `sympy`¹⁶ and converted to a skeleton equation as $f(x) = c_1 \cdot x_1 \cdot x_2^{c_2}$, where c 's are constant tokens¹⁷ and x_1 and x_2 are the first and second variables, respectively.

Table S13 shows the predicted skeleton equations and normalized edit distance from the target skeleton. For the specific true symbolic expression, gplean, AFP, and AFP-FE could not finish the training to produce symbolic expressions for the corresponding tabular data within the session timeout, which is part of our runtime constraints. While the skeleton equation produced by the Symbolic Transformer (ST) is not a perfect solution, it is structurally closer to the target skeleton than those produced by AI Feynman and DSR. It seems that both AI Feynman and DSR attempted to fit the training data and minimize their regression errors, but they resulted in overcomplex symbolic expressions.

Table S14 shows a different example (I.14.3 from Table 1) where some of the other baseline methods performed better than the Symbolic Transformer. While DSR and Symbolic Transformer produced overcomplex or simpler solutions, AFP, AFP-FE, and AI Feynman produced a perfect skeleton with respect to normalized edit distance from the true equation. Overall, our Symbolic Transformer baseline seems to prefer simpler symbolic expressions, that may avoid overcomplex symbolic expressions as a result.

E Injecting Noise to Target Variables

Following SRBench [26], we introduce Gaussian noise with a parameter of noise level γ to the target variables in our SRSD datasets. We inject Gaussian noise to each of the datasets separately, following Eq. (S2):

$$y_j^{\text{noise}} = f_{\text{true}}(X_j) + \epsilon, \quad \epsilon \sim \mathcal{N}\left(0, \gamma \sqrt{\frac{1}{N} \sum_{k=1}^N f_{\text{true}}(X_k)}\right), \quad (\text{S2})$$

where $1 \leq j \leq N$ and N indicates the number of samples in the dataset.

Table S15 shows normalized edit distances of our baselines for noise-injected SRSD (Easy), reusing the set of noise levels in SRBench [26] *i.e.*, $\gamma \in \{0, 10^{-3}, 10^{-2}, 10^{-1}\}$. Interestingly, our Symbolic Transformer (ST) baseline seems less sensitive to noise injected to target variables than other baseline methods. Overall, the more the injected noise is, the more difficult it would be for the baseline models to (re-)discover the physics law in the data.

¹⁶ $E(q_1, r) = \frac{q_1}{4\pi\epsilon r^2} \rightarrow f(x) = 8987742437.98822 \cdot x_1/x_2^2$ by substituting the constant values in Table 1.

¹⁷When computing normalized edit distance, we treat all the constants (c 's) in a skeleton equation as duplicate nodes. *i.e.*, As tree nodes, constant indices are not important since those will be estimated separately at the end, and in general the estimated constant values should not affect the edit distance.

Table S13: An example (I.12.4) that Symbolic Transformer performed better than other baselines.

Target Skeleton	$c_1 \cdot x_1 / x_2^{c_2}$	NED
AI Feynman	$\tan(x_2 / \sqrt{x_2^{c_1}} + c_2)$	1.00
DSR	$x_1 \cdot (x_1 + c_1 \cdot \exp((c_2 \cdot \cos(x_2 + c_3) + c_4) / x_2)) \cdot \exp(-x_2)$	1.00
ST	$c_1 \cdot x_2^{c_2}$	0.167

Table S14: An example (I.14.3) that AFP, AFP-FE, and AI Feynman outperformed ST.

Target Skeleton	$c_1 \cdot x_1 \cdot x_2$	NED
AI Feynman [†]	$c_1 \cdot x_1 \cdot x_2$	0.00
DSR	$x_1 \cdot x_2 \cdot (c_1 - (c_2 \cdot x_2 + c_3 \cdot \log(\cos(x_2))) \cdot (-x_1 + x_2 + c_4) / x_2)$	1.00
ST	$x_1 \cdot x_2$	0.250

[†]AFT and AFP-FE produced exactly the same skeleton with AI Feynman, which resulted in NED = 0.

Table S15: Normalized edit distances of baselines for noise-injected SRSD (Easy) datasets with different noise levels.

Noise Level (γ) \ Method	gplearn	AFP	AFP-FE	AI Feynman	DSR	ST
0	0.876	0.703	0.712	0.646	0.551	0.435
10^{-3}	0.928	0.799	0.814	0.797	0.820	0.435
10^{-2}	0.940	0.824	0.880	0.870	0.793	0.435
10^{-1}	0.948	0.823	0.960	0.882	0.841	0.461

Table S16: Solution rates of common baselines for FSRD and SRSD (Easy, Medium, Hard) datasets.

Dataset \ Method	gplearn	AFP	AFP-FE	AI Feynman	DSR
FSRD [48]	15.5%	20.48%	26.23%	52.65%	19.71%
SRSD (Ours)	1.67%	5.83%	5.83%	9.17%	15.0%

F Solution Rate Comparison - FSRD vs. SRSD -

Table S16 compares the solution rates of the five common baselines for the FSRD and our SRSD datasets. We can confirm that the overall solution rates for our SRSD are significantly degraded compared to those for the FSRD reported in SRBench [26]. The results indicate that our SRSD datasets are more challenging than the FSRD in terms of solution rate.